Quanto option pricing: A joint framework for tempered stable processes and stochastic correlation

A Dissertation presented

by

Hyangju Kim

to

The Graduate School

in Partial Fulfillment of the Requirements

for the Degree of

Doctor of Philosophy

in

Applied Mathematics and Statistics

Stony Brook University

January 2021

Stony Brook University

The Graduate School

Hyangju Kim

We, the dissertation committee for the above candidate for the

Doctor of Philosophy degree, hereby recommend

acceptance of this dissertation

Young Shin Aaron Kim - Dissertation Advisor
Associate Professor, College of Business

James Glimm - Chairperson of Defense
Professor, Applied Mathematics and Statistics

Haipeng Xing - Committee Member
Associate Professor, Applied Mathematics and Statistics

Svetlozar Rachev - External Committee Member
Professor, Department of Mathematics and Statistics, Texas Tech University

This dissertation is accepted by the Graduate School

Eric Wertheimer
Dean of the Graduate School

Abstract of the Dissertation

Quanto option pricing: A joint framework for tempered stable processes and stochastic correlation

by

Hyangju Kim

Doctor of Philosophy

in

Applied Mathematics and Statistics

Stony Brook University

2021

We propose a joint framework combining tempered stable processes with stochastic correlation for quanto option pricing. Most option pricing practices are based on the normal distribution and constant correlation assumptions, thus prone to implied volatility skew and time-varying correlation. To address this discrepancy with the real financial market at-

tributed to the rigid assumptions, we combine two key processes; the normal tempered stable (NTS) process for the underlying dynamics and the Ornstein-Uhlenbeck (OU) process for stochastic correlation to accurately predict quanto option pricing. We label this as the NTS-OU model, in which we compare the results to the NTS model with constant correlation and the classic Black-Scholes model. For its empirical application, we examine the European quanto option valuation and derive its closed-form solution under the risk-neutral measure. We estimate the model performance through two quanto contracts in different market regimes; a quanto option with S&P 500 index and Euro-US dollar exchange rate, and a quanto option with Dow Jones Industrial Average and Bitcoin-US dollar exchange rate. In both examples, the NTS-OU model gives the best estimates due to its flexibility. Building on our experimental findings, we also identify that the stochastic correlation exists in the risk-neutral world.

Dedication Page

To my husband Jisung and my daughter Seohyun

Contents

List of Figures

List of Tables

Acknowledgements

Firstly, I should begin by expressing my deepest gratitude to Professor Young Shin Aaron Kim, who always guided me with immense knowledge and passion during this rewarding journey. His persistent endeavors for mathematical solutions to real-world problems and unwavering enthusiasm kept inspired me to continue to study further. I believe the lesson from him including the knowledge as well as the positive outlook will be a valuable asset throughout my life. Last but not least, his generosity and humor made me enjoy the time spent at Stony Brook University.

My gratitude also extends to my committee members. Professor Svetlozar Rachev's mentoring and encouragement was especially invaluable for me, and he also made helpful comments on the dissertation. I must likewise thank Professor James Glimm and Professor Haipeng Xing whose gave me great insights for the future study. I thank Professor Svetlozar Rachev and Professor James Glimm, in particular, who gave me an opportunity to work as a summer intern at Glimm Analytics. During this internship, I was impressed by their sophisticated philosophy and also their exceptional passion for entrepreneurship. It was one of my best moments at Stony Brook University, and I am grateful for what they have offered me. I would also like to thank Professor Hak Ju Kim who gave me a teaching opportunity at Hofstra University. I also thank my colleagues and mentors. I feel that I was lucky to be surrounded by such talented people and inspired by them.

Finally, I would like to acknowledge my family and parents with sincere gratitude. My special thank firstly goes to my daughter Emma who gave me the greatest joy and strength. My family all kept me going to finish this

long journey and this dissertation could not have been possible without my family's prays, support, and love.

1 Introduction

A quanto option, also referred to as a foreign-equity option, is a cross-currency derivative that the underlying asset is presented in one currency, but settled in a second currency with a pre-determined exchange rate at maturity. As cross-border investments expand,[1] the quanto option receives growing attention from investors seeking to invest in foreign assets without any exposure to currency risk. Indeed, the traditional vanilla quanto derivatives are traded in a significant volume through the over-the-counter market (see Jäckel (2016)).

Accompanying this growth in the market, many studies have been developed pricing models for quanto option. While a quanto option is a convenient financial instrument to eliminate the currency risk, its option premium is not simply to be determined. This is so because the quanto option pricing depends on not only the two underlying assets - the asset price and the foreign exchange rate - but their correlation as well.

The previous approach for quanto option pricing is based on the two-dimensional Black-Scholes (BS) framework (Black and Scholes (1973)) which assumes that the two underlying asset returns follow the lognormal distribution, and the correlation between underlying assets is constant (cf. Black *et al.* (1990), Baxter *et al.* (1996) and Duan and Wei (1999)). However, many studies have pointed out that the BS model fails to explain the two important empirical phenomena: (1) volatility smile and (2) stochastic correlation (see Carr and Wu (2004) and Rachev *et al.* (2005)).

[1] According to the data from SIFMA, the capital market size of United States investing in foreign securities increased by 9.3% from 2018 to $36.9 trillion in 2019. Meanwhile, foreign gross investment in United States securities climbed up 12.7% to $82.1 trillion in 2019.

After Black Monday in 1987, the recognition of the volatility smile has directly motivated studies to investigate the effect of a discrepancy between the BS model and the nature of the real market. The volatility smile reflects a smile pattern shown when implied volatility is plotted against strike prices. However, the assumption of the lognormal distribution of the asset returns leads to constant volatility instead of a 'skewed' smile. This distortion arises because the empirical distribution of the underlying asset returns exhibits heavy tails, and skewness; the lognormal distribution displays the symmetric and rapidly decaying tails which is not consistent with these stylized facts (cf. Rachev and Mittnik (2000) and Mittnik *et al.* (2000a)). Hence, the BS model undervalues out-of-the-money options, whereas in-the-money options and at-the-money options are assessed at a higher price to compensate for it.

Many subsequent models have been proposed to tackle this volatility smile phenomenon and one milestone approach is replacing the lognormal distribution with the tempered stable (TS) distribution. The tails of the TS distribution are 'tempered', so it shows heavier tails than the normal distribution. In addition to this, its parameters also capture the skewness as well as the mean and the variance. Because of this flexibility, the TS distribution better explains the realities of real-world movement of the underlying asset returns and, thus, it became the most suitable alternative to price derivatives.

The TS distribution was firstly introduced by Koponen as "truncated Lévy flights" (Koponen (1995)). Later, its extensions are suggested as: "KoBoL" (Boyarchenko and Levendorskii (2000)), "CGMY" (Carr *et al.* (2002)), "KR" (Kim *et al.* (2008) and Kim *et al.* (2009)), "Modified Tempered Stable" (Kim (2005) and Kim *et al.* (2006)), and "Smoothly Truncated Stable"

(Menn and Rachev (2009)). The TS distribution has six types of a well-known subclass, and we employ the normal tempered stable (NTS) distribution for our study.

The NTS distribution is proposed by Barndorff-Nielson and Shepard (Barndorff-Nielsen *et al.* (2001)), and it defines a time-changed Brownian motion with a tempered stable subordinator. Basically, the NTS distribution evaluates the Brownian motion at a random time instead of physical time (or real-time). The random time is referred to as the *subordinator* or *intrinsic time process*. More specifically, it is constructed by an exponential tilting of Lévy measure, and the procedure of tilting is from the Esscher transform (Gerber and Shiu (1994)). Since the NTS distribution is developed aiming for more flexible modeling possibilities that capture the observed features in the real world, in terms of this, the NTS distribution has an obvious benefit over the normal distribution.

However, the studies on the quanto option based on the NTS distribution have been relatively sparse. The first work beyond the BS framework is Huang and Hung (2005) which applied the Lévy process for quanto option pricing. Recently, Kim *et al.* (2015) formulated a NTS-based pricing model and derived its closed-form solution. Still, the correlation between the two underlying processes remained constant in this model. The motivation of our study is to expand the constant correlation as the stochastic correlation under the NTS framework to address the second drawback of the BS model as we discussed.

It is a well-documented fact that the stochastic correlation plays a key role in the pricing of multi-asset financial instruments (Teng *et al.* (2015)). However, much of the studies assume it as constant due to its computational ease despite its importance. Indeed, using a constant correlation could

encounter two critical problems from practitioner's view: (1) Estimating a correlation is largely affected by the timeframe. Hence, deciding the timeframe in practice can be a tricky problem and it may mislead the true estimates, which can be more noticeable when the market is in distress and needs the correct estimates most. (2) The implied correlation derived from the market data is not consistent with the realized correlation and this implies the non-zero correlation risk premium (see Ma (2009) and Linders and Schoutens (2014)).

In our study, we utilize the Ornstein-Uhlenbeck (OU) process to describe the stochastic correlation. The OU process is a stationary Gauss-Markov process, and has two useful properties that make the OU process easy to work with; the mean-reverting and the positive definite variance-covariance matrix. For this reason, the OU process has gained popularity to describe the stochastic correlation.

In the following, we establish a general framework for quanto option pricing by incorporating the NTS process and the OU process. We assume that the dynamics of underlying assets are governed by a NTS process, and the stochastic correlation between underlying assets is described by the OU process. We name this model the NTS-OU. We also derive its closed-form solution under the risk-neutral measure. As a general framework, the NTS-OU model encompasses the BS model and the previous NTS framework with constant correlation. To change physical measure to risk-neutral measure $\mathbb{Q}$, we apply the Girsanov's Theorem (cf. Theorem 10.8, Klebaner (2005)) and find the *Radon-Nikodym derivative*.

For our empirical illustration, we set up two quanto option contracts to show that the NTS-OU model works in the two different market regimes: (1) a quanto contract with the S$P 500 index and the Euro-US Dollar

(EUR-USD) exchange rate and (2) a quanto option with the Dow Jones Industrial Average index with the Bitcoin-US Dollar (BTC-USD) exchange rate. The calibration results show that the NTS-OU model provides the best estimates for the option price compared to the BS model or the NTS model with constant correlation. This is supported by the lowest RMSE, AAE, and APE. Also, another important inference is that we confirm the existence of stochastic correlation in the risk-neutral world based on the comparison with the NTS model with constant correlation and the NTS-OU model.

The study of Bitcoin quanto contract is more interesting in particular because the derivatives market is expanding for cryptocurrencies recently. In July 2020, the EQUOS is set to be the first US publicly trading exchange for cryptocurrencies with further plans to list perpetual swaps, futures, options, and other derivatives products soon. In addition to this, the trading volume of the cryptocurrency derivatives for the second quarter of 2020 was \$2.159 trillion, a 2.57% increase from the first quarter according to Tokeninsight. Statistics around the cryptocurrency derivatives market indicate that the market keeps growing at an exponential rate. With this new era coming, the NTS-OU model can facilitate the use of the cryptocurrency quanto option by providing the most accurate price. As we examine in the empirical part, the NTS and the OU assumptions allow us to capture the volatile movement of cryptocurrency the best.

This paper is organized as follows. In section 2, we revisit the preliminary properties of the NTS process and the OU process. Section 3 describes the NTS-OU framework, and applies this framework to quanto option pricing in Section 4. Empirical study is presented in Section 5. Section 6 offers a conclusion.

2 Preliminaries

Before we proceed to the construction of our quanto option pricing model, we revisit important stochastic processes and numerical calculation techniques that are used for our study: the Lévy process, the TS process, the NTS process, the OU process, and the fast Fourier transform (FFT) method.

In this section, we explore the definition and properties of each process as well as the relationship of the processes. We begin with the definition of the Lévy process and discuss the empirical facts that the Lévy process is capable of characterizing. We also present the variety of subclasses within the definition of the Lévy process mainly focusing on the TS process. By exploring its well-known subclasses, we illustrate how rich a class of processes they form.

We note that the NTS-OU model is constructed by incorporating the NTS and the OU processes. The NTS process models the marginal distribution capturing empirical properties such as jumps, heavy tails, and skewness. The OU process describes the stochastic correlation between the underlying asset and the exchange rate by assuming the correlation to follow a stationary Markov process. With these two processes, we derive their analytical formula for the quanto option pricing under the risk-neutral measure, $\mathbb{Q}$.

2.1 Lévy process

The Lévy process is a continuous stochastic process named after Paul Lévy who first introduced the class of non-Gaussian stable distributions. The Lévy process has played an instrumental role in probability theory and

financial modeling due to its properties; independent increments, stationary increments, infinite divisibility, and finite moments. These properties are advantageous in describing the dynamics of asset return which exhibits jumps, heavy tails, and skewness. The Gaussian process utilizes only two parameters, for this reason, it has a clear limitation to describe the true behavior of the real market. As a result, the Lévy process with more flexibility has emerged as the alternative, Mandelbrot (1963) introduced the first application of the Lévy process for the asset price process. Much of the subsequent studies has been proposed for more general reference of Lévy process by Bertoin (1996), Ken-Iti (1999), and Cont and Tankov (2004).

Before we continue with the discussion of and the construction of the Lévy process, we define the Lévy process first.

Definition 1 (Lévy Process)**.** *A stochastic process $X = \{X_t\}_{t\geq 0}$ is said to be a Lévy process if the following conditions are satisfied:*

1. $X(0) = 0$, *a.s.*
2. X *has independent increments.*
3. X *has stationary increments.*
4. X *is right continuous with left limits.*
5. X *is stochastically continuous,* $\forall t \geq 0$ *and* $a > 0$,

$$\lim_{s\to t} P[|X_s - X_t| > a] = 0.$$

The characteristic function of a Lévy process is written by the Lévy - Khintchine formula (also can be applied to the general *infinitely divisible*

distributions):

$$exp\left(i\gamma u - \frac{1}{2}\sigma^2 u^2 + \int_{-\infty}^{\infty}(e^{iux} - 1 - iux1_{|x|\leq 1})\nu(dx)\right). \tag{2.1}$$

In the formula, the ν is called as the *Lévy measure* which is one of a Borel measure if $\nu(0) = 0$ and $\int_{\mathbb{R}}(1 \bigwedge |x^2|)\nu(dx) < \infty$. The triplet ($\sigma^2$, ν, γ) is referred to as a *Lévy triplet* where $\sigma, \nu \in \mathbb{R}$, and $\sigma \geq 0$. The derivation of this formula is given in Ken-Iti (1999). We note that a infinitely divisible distributions was proposed by Kolmogorov in case of the second moments of the Lévy –Khintchine formula.

Meanwhile, the Lévy process can be divided into two main parts; a Brownian motion and a pure jump rocess $(Z_t)_{t\geq 0}$. That is

$$X_t = \sigma W_t + Z_t \tag{2.2}$$

and using this formula, we can obtain the characteristic function of Lévy process X_t as follows:

$$\begin{aligned}
\phi X_t(u) &= \phi_{\sigma W_t(u)}\phi_{Z_t(u)} \\
&= exp\left(-\frac{t}{2}\sigma^2 u^2\right) exp\left(i\gamma ut + t\int_{-\infty}^{\infty}(e^{iux} - 1 - iux1_{|x|\leq 1})\nu(dx)\right) \\
&= exp\left(i\gamma ut - \frac{t}{2}\sigma^2 u^2 + t\int_{-\infty}^{\infty}(e^{iux} - 1 - iux1_{|x|\leq 1})\nu(dx)\right)
\end{aligned} \tag{2.3}$$

where $\phi_{\sigma W_t(u)}$ is the characteristic function of $N(0, \sigma^2 t)$ and $\phi_{Z_t(u)}$ is the

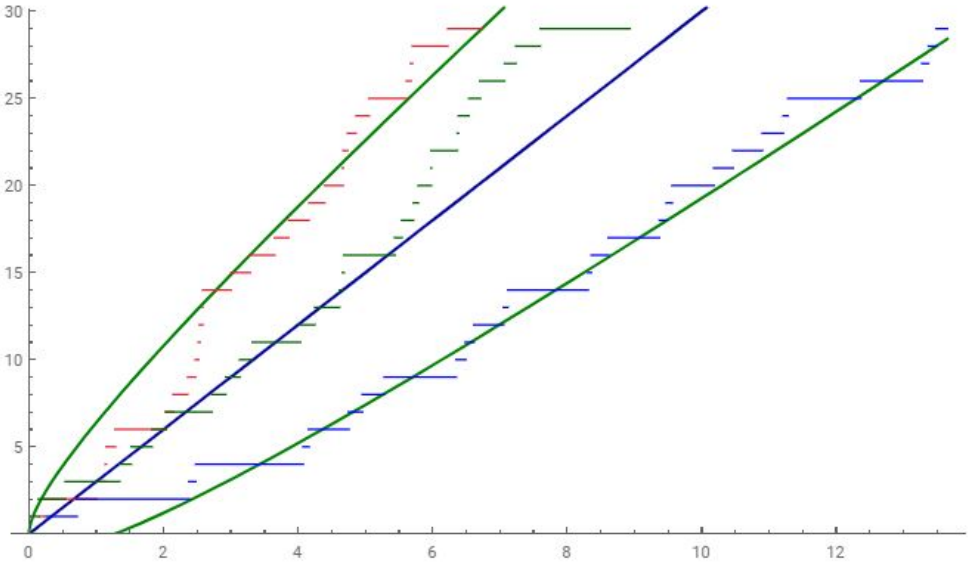

Figure 1: A sample path of a Poisson process with $\lambda = 3$. With the same mean, three different paths are shown.

characteristic function of the pure jump process, that is

$$\phi_{Z_t(u)} = exp\left(i\gamma ut + t\int_{-\infty}^{\infty}(e^{iux} - 1 - iux1_{|x|\leq 1})\nu(dx)\right). \tag{2.4}$$

As we can see in equation 2.2, the standard Brownian motion and pure jump processes all belong to the Lévy process. Now, we proceed to discuss some well-known examples of the Lévy process which give us the impression of how varied the class of Lévy process really is and how the properties of the Lévy process contribute to capturing the stylized facts of the nature of the real market movement.

2.1.1 Poisson process

A process valued on the non-negative integers $N = (N_t)_{t\geq 0}$ defined on a probability space $(\omega, \mathcal{F}, \mathcal{P})$ is referred to as a Poisson process with intense

parameter λ as follows:

1. $N_0 = 0$
2. N has independent and stationary increments.
3. For $s \geq 0$ and $h \geq 0$, $N_{t+h} - N_t$ is a Poisson distributed random variable with parameter λh if satisfy,

$$\mathbb{P}(N_{t+h} - N_t = n) = e^{-\lambda h}\frac{(\lambda h)^n}{n!}.$$

The characteristic function of the Poisson process is given by

$$\phi_{N_t}(u) = E(e^{iuN_t}) = e^{\lambda t(1-e^{iu})}. \tag{2.5}$$

The Poisson process is a fundamental building block of pure jump process which is a main component of the Lévy process in equation 2.2.

2.1.2 Pure jump process

A process $X^x = (X_t^x)_{t\geq 0}$ for a real number x follows

$$(X_t^x) = xN_t^{\lambda(x)}$$

and $(N_t^{\lambda(x)})_{t\geq 0}$ is the Poisson process with parameter $\lambda(x)$. x is a given number which means the jump size, and the intensity parameter $\lambda(x)$ is the expected number of jumps in the unit time interval.

Using this notation, we construct a process Y_t is defined by

$$Y_t = \gamma t + \sum_{j=1}^{\infty} X_t^{x_j}.$$

Recall that X_t^x follows the Poisson process, the characteristic function of

X_t^x is written in the form of 2.5, and that is,

$$\phi_{X_t^x}(u) = exp\left(\lambda(x)t(e^{iux} - 1)\right). \tag{2.6}$$

By plugging the notation of Y_t into equation 2.6, we derive the characteristic function of Y_t as follows:

$$\phi_{Y_t} = exp\left(i\gamma ut + t\sum_{j=1}^{\infty}\lambda(x_j)(e^{iux_j} - 1)\right).$$

Now, we assume that the jump size can be any real number. Under this assumption, we can denote the expected number of jump size as $\nu([a,b])$, and we rewrite the characterisric function of Y_t,

$$\phi_{Y_t} = exp\left(i\gamma ut + t\int_{-\infty}^{\infty}(e^{iux} - 1)\nu(dx)\right) \tag{2.7}$$

where $\gamma \in \mathbb{R}$ and we call the measure ν as a Lévy measure. So far, we call the process of Y_t is a jump process.

However, there is a major drawback for the equation 2.7; infinite variation of process cannot be embedded in this framework. To take account for this property, we define another process Z_t which the characteristic function is given by

$$\phi_{Z_t} = exp\left(i\gamma ut + t\int_{-\infty}^{\infty}(e^{iux} - 1 - iux1_{|x|\leq 1})\nu(dx)\right) \tag{2.8}$$

and finally we obtain the pure jump process. We note that the pure jump process is the modification of the Poisson process. Hence, it inherits the properties of the Poisson process as well.

The pure jump process has many subclasses in it, for example, gamma process, inverse Gaussian process, variance gamma process, α-stable process, TS process, and so on. We briefly point out the definition and the properties of the TS process in the next section.

2.1.3 TS process

A Tempered stable processes were introduced as the truncated Lévy flight (Koponen (1995)) model in physics literature, and later, it is applied to model stochastic volatility, for example, the CGMY model (see Carr *et al.* (2002) and Carr *et al.* (2003)), or the Ornstein-Uhlenbeck–based model (see Barndorff-Nielsen and Shephard (2001) and Barndorff-Nielsen *et al.* (2001)).

The construction of the tempered stable processes is mixing up the α–stable process and the Gaussian trends. Hence, in a short-term view, it approaches to an α–stable process while in a long-term view, it close to a Brownian motion (see Rosiński (2007)). In addition to this, the TS distribution is obtained by 'tempering' the tails, so it represents the heavier tails than the normal distribution. The Skewness and jumps are also described by flexible shape of the TS process.

The TS process has largely six subclass such as the classical tempered stable (CTS) process, the generalized tempered stable (GTS) process, the modified tempered stable (MTS) process, the normal tempered stable (NTS) process, the normal inverse Gaussian (NIG) process, the Kim-Rachev tempered stable (KRTS) process, and the rapidly decreasing tempered stable (RDTS) process. We employ the NTS process in particular to build our model.

2.1.4 Time-changed Brownian motion

The Brownian motion is well-known stochastic process in Finance. We start with the definition of the Brownian motion.

Definition 2 (Brownian Motion)**.** *A standard Brownian motion* $W = (W_t)_{t\geq 0}$ *is satisfying the conditions as follows:*

1. $W_0 = 0$

2. W has independent and stationary increments.

3. The increments of $W_{t+h} - W_t$ *follows the normal random variable with mean zero and variance* h*.*

4. The paths are continuous.

Now, we consider a pure jump process $T = (T_t)_{t\geq 0}$ which present nondecreasing trajectory, then the process T can be utilized to represent a trading executed time instead of physical time. (see Mittnik *et al.* (2000b)). In this case, the process T is called as the subordinator or intrinsic time process.

If we consider an arithmetic Brownian motion and set the subordinator instead of the physical time, we obtain define the time-changed Brownian motion as follows:

$$X_t = \mu T_t + \sigma W_{T_t}.$$

The characteristic function of the time-changed Brownian motion is given by

$$\phi_{X_t}(u) = \phi_{T_t}\left(\mu u + \frac{iu^2\sigma^2}{2}\right). \tag{2.9}$$

Based on the contribution of Monroe (1978), we know that every semimartingale can be written as a form of the time-changed Brownian motion. Moreoever, theoretically, every Lévy processes can be represented as

Time-changed Brownian Motion (see Clark (1973)). This property of the Lévy process makes the best alternative process to describe the true dynamics of the market.

One drawback is that it is not easy to represent the time-change explicitly. To address this problem, many subsequent models are suggested and the best known is the CGMY process introduced by Carr *et al.* (2002) and the Meixner process which is proposed by Grigelionis (1999) and Schoutens (2002). Recently, Madan and Yor (2006) described the CGMY and Meixner processes as time changed Brownian motions from.

2.2 NTS process

Let $\alpha \in (0,2)$, $\theta, \sigma > 0$, and $\mu, \beta \in \mathbb{R}$. The NTS random variable X with parameters $(\alpha, \theta, \beta, \sigma, \mu)$ is defined as

$$X = \mu - \beta + \beta\mathcal{T} + \sigma\sqrt{\mathcal{T}}W,$$

where $W \sim \mathrm{N}(0,1)$, $\mathcal{T}$ is a positive, non-decreasing random variable called *tempered stable subordinator* with its characteristic function $\phi_{\mathcal{T}}$ being

$$\phi_{\mathcal{T}}(u) = \exp\left(-\frac{2\theta^{1-\frac{\alpha}{2}}}{\alpha}((\theta - iu)^{\frac{\alpha}{2}} - \theta^{\frac{\alpha}{2}})\right).$$

Now finally, the characteristics function of X is given by

$$\phi_{NTS}(u) = E[e^{iuX}] = \exp\left((\mu-\beta)iu - \frac{2\theta^{1-\frac{\alpha}{2}}}{\alpha}\left(\left(\theta - i\beta u + \frac{\sigma^2 u^2}{2}\right)^{\frac{\alpha}{2}} - \theta^{\frac{\alpha}{2}}\right)\right). \tag{2.10}$$

N-dimensional NTS process has the following parameters: $\alpha \in (0,2)$,

$\theta > 0$, $\mu = (\mu_1, \mu_2, \cdots, \mu_N)^T \in \mathbb{R}^N$, $\beta = (\beta_1, \beta_2, \cdots, \beta_N)^T \in \mathbb{R}^N$ and $\sigma = (\sigma_1, \sigma_2, \cdots, \sigma_N)^T$ with $\sigma_n > 0$, for all $n \in 1, 2, \cdots, N$. $R = [\rho_{m,n}]_{\{m,n \in 1,2,\cdots,N\}}$ is a dispersion matrix and $R^{\frac{1}{2}}$ given by factorization $R = R^{\frac{1}{2}}(R^{\frac{1}{2}})^T$ such as a Cholesky factorization. Note that α determines fat-tailedness and peakedness as well as the jump intensity where $\alpha \in [1, 2)$ implies infinite variation and $\alpha \in (0, 1)$ implying finite variation. θ is the tempering and scaling parameter for the subordinator, μ is the drift of the NTS process.

Let $(\mathcal{T}(t))_{t \geq 0}$ be the tempered stable subordinator generated by the infinitely divisible $\mathcal{T}$ and $(W(t))_{t \geq 0}$ be an independent N-dimensional Brownian motion independent of the subordinator. Then an N-dimensional process $(X(t))_{t \geq 0}$ follows the multivariate NTS if

$$X(t) = \mu t + \beta(\mathcal{T}(t) - t) + \text{diag}(\sigma) R^{\frac{1}{2}} W(\mathcal{T}(t)), \quad t \geq 0$$

and denoted by $X \sim NTS_N(\alpha, \theta, \mu, \beta, \sigma, R)$. For each $n \in \{1, 2, \cdots, N\}$, the characteristic function defining its marginal distribution of X_n is

$$\phi_{X_n(t)}(u) = \exp\left((\mu_n - \beta_n) iut - \frac{2t\theta^{1-\frac{\alpha}{2}}}{\alpha} \left(\left(\theta - \beta_n iu + \frac{\sigma_n^2 u^2}{2} \right)^{\frac{\alpha}{2}} - \theta^{\frac{\alpha}{2}} \right) \right),$$

and the expectation of this is given as $E[X_n(t)] = \mu_n t$ and the covariance is

$$\text{cov}(X_m(t), X_n(t)) = \sigma_m \sigma_n \rho_{m,n} t + \beta_m \beta_n t \left(\frac{2 - \alpha}{2\theta} \right). \tag{2.11}$$

Note that, the characteristic function is also analytically specified in the complex field which implicates that if $\xi \in I_n$, then $\phi_{X_n(t)}(\xi)$ is well defined.

$$I_n = \left\{ z \in \mathbb{C} : -\frac{1}{\sigma_n^2} \left(\beta_n + \sqrt{\beta_n^2 + 2\sigma_n^2 \theta} \right) \leq \text{Im}(z) \leq \frac{1}{\sigma_n^2} \left(\sqrt{\beta_n^2 + 2\sigma_n^2 \theta} - \beta_n \right) \right\}.$$

2.3 OU process

We model the stochastic dependency with the OU process. The OU model is the Gauss-Markov process, and also it is a continuous case of the AR(1) model. The OU process has bounded variance and stationary probability distribution as opposed to the Wiener process which is not a stationary process. This comes from the fact that the Wiener process has a constant drift term, whereas the OU process has a drift that is dependent on its current level of the process. In other words, if the value of the process is less than the long term mean, the drift gradually moves towards a positive direction and vice versa. This gives the process the mean-reverting property which is important to describe the stochastic correlation.

Let θ be the long-term mean, κ be the reverting speed of the process, and σ be the volatility of the stochastic process. A stochastic process $X(t)$ follows the OU process if the dynamic is as below:

$$dX_{(t)} = -\kappa(X_{(t)} - \theta)dt + \sigma dW(t);$$

where $W(t)$ is a standard Brownian motion. For our study, in particular, we assume the long-term mean θ is zero and the correlation movement in $\mathbb{Q}$-measure is explained by the drift and the Brownian motion part.

2.4 Fourier transform and characteristic function

For a given function $f(x)$, its Fourier transform is defined as

$$\Phi(\nu) = \int_{-\infty}^{\infty} e^{i\nu x} f(x)dx.$$

This is transforming a given function into the frequency space where the function gets decomposed into harmonic functions. The Fourier transform of a function, $\Phi(\nu)$, can then easily be recovered by the inverse Fourier transform,

$$f(x) = \frac{1}{2\phi} \int_{-\infty}^{\infty} e^{-i\nu x} \Phi(\nu) d\nu.$$

If $f(x)$ is a given probability density function (pdf) of a random variable x, this Fourier transform of the pdf is called characteristic function,

$$\begin{aligned} \Phi(\nu) &= \int_{-\infty}^{\infty} e^{i\nu x} f(x) dx \\ &= \mathbb{E}(e^{i\nu x}), \end{aligned}$$

and as explained pdf $f(x)$ can be recovered from its characteristic function.

Characteristic functions can be used to calculate the moments of a given distribution function. The number of moments of that distribution can be calculated as follows. Suppose we have the characteristic function of a random variable X as

$$\phi(u) = \mathbb{E}[e^{iuX}].$$

By calculating the nth derivative of $\phi(u)$ we can get the following expression

$$\phi^{(n)}(u) = \mathbb{E}[(iX)^n e^{iuX}].$$

Now to find its moments, we can plug in zero for u and obtain,

$$\begin{aligned}\phi^n(0) &= \mathbb{E}\left[(iX)^n e^{i(0)X}\right] \\ &= \mathbb{E}\left[(iX)^n\right] \\ &= i^n \mathbb{E}\left[X^n\right].\end{aligned}$$

Therefore,

$$\mathbb{E}[X^n] = i^{-n}\phi^n(0).$$

For example, if the first moment of X, i.e. the mean, is to be calculated then:

$$\mathbb{E}[X] = -i\phi^{'(0)}.$$

Now we examine one example to understand how a characteristic function is being calculated given a pdf. We use standard normal distribution as an example. One of the most widely known and important distribution is the standard normal distribution. This is used in many applications including various spaces in the financial industry. Albeit it's disadvantage of not capturing skew and tailedness, it is the building block of diffusion process and thus is absolutely central to most of the theories.

If $Z \sim \mathcal{N}(0,1)$, then its characteristic function is calculated as

$$\Phi_Z(\nu) = \mathbb{E}(e^{i\nu Z}) = \int_{-\infty}^{\infty} \frac{1}{\sqrt{2\pi}} \exp\left(i\nu z - \frac{1}{2}z^2\right) dz.$$

Now note that,

$$\mathbb{E}(e^{sZ}) = \int_{-\infty}^{\infty} \frac{1}{\sqrt{2\pi}} \exp\left(sz - \frac{1}{2}z^2\right) dz.$$

Calculate the integrand as follows

$$\begin{aligned}\int_{-\infty}^{\infty}\frac{1}{\sqrt{2\pi}}\exp\left(sz-\frac{1}{2}z^2\right)dz &= \int_{-\infty}^{\infty}\frac{1}{\sqrt{2\pi}}\exp\left(-\frac{1}{2}(z^2-2sz)\right)dz\\ &= \int_{-\infty}^{\infty}\frac{1}{\sqrt{2\pi}}\exp\left(-\frac{1}{2}(z-s)^2+\frac{1}{2}s^2\right)dz\\ &= \frac{1}{\sqrt{2\pi}}e^{\frac{1}{2}s^2}\int_{-\infty}^{\infty}\exp\left(-\frac{1}{2}(z-s)^2\right)dz,\end{aligned}$$

now as the following holds:

$$\int_{-\infty}^{\infty}e^{-\frac{1}{2}u^2du}=\sqrt{2\pi},$$

we can get

$$\mathbb{E}(e^{sZ})=\exp\left(\frac{s^2}{2}\right).$$

By substituting $i\nu$ for s we can get

$$\Phi_Z(\nu)=\mathbb{E}(e^{i\nu Z})=e^{-\frac{\nu^2}{2}}.$$

3 NTS processes with stochastic correlation

In this section, we extend the NTS framework with the stochastic correlation. We apply Girsanov's theorem to change measure from the physical measure $\mathbb{P}$ to the risk-neutral measure $\mathbb{Q}$. Subsequently, we look into a bivariate case as a quanto option has two underlying risk factors and derives its characteristic function that is directly leveraged into the pricing.

We follow the same notation used in the previous section 2.2 with R being time-dependent, $R=(R(t))_{t\geq 0}$. Let $\mathcal{T}(t)$ be a tempered stable subordinator and $(W(t))_{t\geq 0}$ be an independent N-dimensional Brownian motion.

Let process $(\tau(t))_{t\geq 0}$ satisfy $\mathcal{T}(t) = \int_0^t \tau(u)du$, for all $t \geq 0$. Then the processes become the following

$$X(t) = \mu t + \beta \int_0^t (\tau(u) - 1)du + \text{diag}(\sigma) \int_0^t R^{1/2}(\mathcal{T}(u))\sqrt{\tau(u)}dW(u) \quad (3.1)$$

and denoted by $X \sim NTS_{OU}(\alpha, \theta, \mu, \beta, \sigma, R)$. Note that the explicit dynamics of our choice for the correlation is not yet specified and this is will be discussed in section 4.3 with the exact pricing formula. For each $n \in \{1, 2, \cdots, N\}$, the characteristic function defining its marginal distribution of X_n is

$$\phi_{X_n(t)}(u) = \exp\left((\mu_n - \beta_n)iut - \frac{2t\theta^{1-\frac{\alpha}{2}}}{\alpha}\left(\left(\theta - \beta_n iu + \frac{\sigma_n^2 u^2}{2}\right)^{\frac{\alpha}{2}} - \theta^{\frac{\alpha}{2}}\right)\right)$$

and the expectation of this is given as $E[X_n(t)] = \mu_n t$ and the covariance is

$$\text{cov}(X_m(t), X_n(t)) = \sigma_m \sigma_n E\left[\int_0^{\mathcal{T}(t)} \rho_{m,n}(s)ds\right] + \beta_m \beta_n t\left(\frac{2-\alpha}{2\theta}\right). \quad (3.2)$$

In addition, it is important to note that a weighted sum of the NTS-OU processes again follows the NTS-OU distribution as the following proposition states.

Proposition 1. *Let* $w = (w_1, w_2, ..., w_N)^\intercal \in \mathbb{R}^N$ *and* N*-dimensional processes* $X \sim NTS_{OU}(\alpha, \theta, \mu, \beta, \sigma, R)$.

$$w^T X(t) = \bar{\mu} t + \bar{\beta}(\mathcal{T}(t) - t) + \int_0^{\mathcal{T}(t)} \bar{\sigma}(s)dW(s), \quad t \geq 0$$

Then $w^T X \sim NTS_{OU}(\alpha, \theta, \bar{\mu}, \bar{\beta}, \bar{\sigma}, R)$

$$\bar{\mu} = \sum_{n=1}^{N} w_n \mu_n, \quad \bar{\beta} = \sum_{n=1}^{N} w_n \beta_n, \quad \bar{\sigma}(t) = \sqrt{\sum_{m=1}^{N}\sum_{n=1}^{N} w_m w_n \sigma_m \sigma_n \rho_{m,n}(t)}$$

where $(W(t))_{t\geq 0}$ *is a Brownian motion.*

This property significantly helps the analytical formula to be simple yet effective as can be seen in the following sections (e.g. section 3.2, section 4) in the derivation of the equations.

3.1 Equivalent martingale measure

In this section, we change the NTS-OU processes into the risk-neutral $\mathbb{Q}$-measure with Girsanov's theorem. We start with stating the theorem by having a probability space $(\Omega, \mathcal{F}, \mathbb{P})$ and a random variable Z which is nonnegative and $E(Z) = 1$.

Theorem 3.1 (Girsanov)**.** *Let* $B(t)$, $0 \leq t \leq T$, *be a Brownian motion on a probability space* $(\Omega, \mathcal{F}, \mathbb{P})$, *and let* $\mathcal{F}(t)$, $0 \leq t \leq T$ *be a filtration for this Brownian motion. Let* $H(t)$, $0 \leq t \leq T$ *be an adopted process. Define*

$$Z(t) = \exp\left(-\int_0^t H(u)dW(u) - \frac{1}{2}\int_0^t H^2(u)du\right),$$

$$W(t) = B(t) + \int_0^t H(u)du,$$

and assume that

$$\mathbb{E}\left[\int_0^T H^2(u)Z^2(u)du\right] < \infty.$$

Set $Z = Z(t)$, then $E(Z) = 1$ and under the probability measure $\mathbb{Q}$ given by

$$\mathbb{Q}(A) = \int_A Z(\omega) dP(\omega) \ for \ all \ A \in \mathcal{F},$$

the process $W(t)$, $0 \leq t \leq T$, is a Brownian motion.

Now, let's apply the theory to the multivariate NTS equation 3.1 with stochastic correlation. In order to change the measure, we define a set of two parameter vectors as $\lambda = (\lambda_1, \lambda_2, \cdots, \lambda_N)$ and $\hat{\beta} = (\hat{\beta}_1, \hat{\beta}_2, \cdots, \hat{\beta}_N)$ that satisfies $\mu - \beta = \lambda - \hat{\beta}$. Along with this, we define an N-dimensional process $H(t) = \big(H_1(t), H_2(t), ..., H_N(t)\big)$ that satisfies the following,

$$\text{diag}(\sigma) R^{1/2}(\mathcal{T}(t)) H(t) = (\beta - \hat{\beta}) \sqrt{\tau(t)}.$$

With λ, $\hat{\beta}$ and $H(t)$ the equation 3.1 becomes,

$$\begin{aligned} X(t) &= \lambda t + \hat{\beta} \int_0^t (\tau(u) - 1) du \\ &\quad + \text{diag}(\sigma) \left(\int_0^t R^{1/2}(\mathcal{T}(u)) \sqrt{\tau(u)} H(u) du + \int_0^t R^{1/2}(\mathcal{T}(u)) \sqrt{\tau(u)} dB(u) \right). \end{aligned}$$

By theorem 3.1, we have the *Radon-Nikodym derivative*

$$\frac{d\mathbb{Q}}{d\mathbb{P}} = e^{\Xi(T) - \frac{1}{2}[\Xi, \Xi](T)} \quad \text{for} \quad \Xi(t) = -\sum_{n=1}^{N} \int_0^t H_n(s) dB_n(s) \tag{3.3}$$

and we also get a process $W(t)$ as below that is a brownian motion under $\mathbb{Q}$-measure

$$W(t) = B(t) + \int_0^t H(u) du.$$

Now we summarize the equation with respect to the new Brownian motion

$W(t)$ as follows:

$$\begin{aligned} X(t) &= \lambda t + \hat{\beta}\int_0^t (\tau(u)-1)du + \mathrm{diag}(\sigma)\int_0^t R^{1/2}(\mathcal{T}(u))\sqrt{\tau(u)}dW(u) \\ &= \lambda t + \hat{\beta}(\mathcal{T}(t)-t) + \mathrm{diag}(\sigma)\int_0^t R^{1/2}(\mathcal{T}(u))dW(\mathcal{T}(u)) \\ &= \lambda t + \hat{\beta}(\mathcal{T}(t)-t) + \mathrm{diag}(\sigma)\int_0^{\mathcal{T}(t)} R^{1/2}(u)dW(u). \end{aligned}$$

$X \sim \mathrm{NTS}_{OU}\left(\alpha, \theta, \lambda, \hat{\beta}, \sigma, R\right)$ under $\mathbb{Q}$-measure with the new set of parameters which is also reiterated and summarized into the following proposition.

Proposition 2. *Suppose* $X \sim \mathrm{NTS}_{OU}(\alpha, \theta, \mu, \beta, \sigma, R)$ *under measure* $\mathbb{P}$. *Let* $\lambda = (\lambda_1, \lambda_2, \cdots, \lambda_N)^\intercal$ *and* $\hat{\beta} = (\hat{\beta}_1, \hat{\beta}_2, \cdots, \hat{\beta}_N)^\intercal$ *be vectors satisfying* $\mu - \beta = \lambda - \hat{\beta}$. *Then, there is an equivalent measure* $\mathbb{Q}$, *such that*

$$X \sim \mathrm{NTS}_{OU}\left(\alpha, \theta, \lambda, \hat{\beta}, \sigma, R\right).$$

In this case, the Radon-Nikodym derivative is given by equation (3.3).

3.2 Bivariate case

In this section, we discuss a two-dimensional case in particular as the application to the quanto option requires modeling the two following risk factors: the exchange rate and the underlying asset. Here we derive the characteristic function of the weighted sum of the two NTS-OU processes, which is subsequently used for the option valuation via Fourier transform.

Let two-dimensional stochastic process follow the bivariate NTS-OU as, $X = (X_1, X_2)^\intercal \sim \mathrm{NTS}_{OU}(\alpha, \theta, \mu, \beta, \sigma, R)$ with parameters to be $\alpha \in (0, 2)$,

$\theta > 0$, $\mu = (\mu_1, \mu_2)^\intercal$, $\beta = (\beta_1, \beta_2)^\intercal$, $\sigma = (\sigma_1, \sigma_2)^\intercal$, $R = (R(t))_{t\geq 0}$ and

$$R(t) = \begin{pmatrix} 1 & \rho(t) \\ \rho(t) & 1 \end{pmatrix}$$

where correlation $\rho = (\rho(t))_{t\geq 0}$ is a time-dependent stochastic process bounded in $[-1, 1]$. Then we have $X(t) = (X_1(t), X_2(t))^\intercal$ with

$$\begin{pmatrix} X_1(t) \\ X_2(t) \end{pmatrix} = \begin{pmatrix} \mu_1 \\ \mu_2 \end{pmatrix} t + \begin{pmatrix} \beta_1 \\ \beta_2 \end{pmatrix} (\mathcal{T}(t) - t) + \begin{pmatrix} \sigma_1 & 0 \\ 0 & \sigma_2 \end{pmatrix} \int_0^{\mathcal{T}(t)} \begin{pmatrix} 1 & 0 \\ \rho(t) & \sqrt{1-\rho(t)^2} \end{pmatrix} \begin{pmatrix} dB_1(t) \\ dB_2(t) \end{pmatrix},$$

where $\mathcal{T}$ is again the tempered stable subordinator, $B = (B(t))_{t\geq 0}$ is the independent two-dimensional Brownian motion, and B, $\mathcal{T}$ and ρ are mutually independent. For the variance and covariance for the two processes, by (3.2), we have

$$(X_j(t)) = \sigma_j^2 t + \beta_j^2 t \left(\frac{2-\alpha}{2\theta}\right) \text{ for } j = 1, 2,$$

and

$$\operatorname{cov}(X_1(t), X_2(t)) = \sigma_1\sigma_2 E\left[\int_0^{\mathcal{T}(t)} \rho(s)ds\right] + \beta_1\beta_2 t \left(\frac{2-\alpha}{2\theta}\right).$$

It is important to reemphasize here that as described in Proposition 1, the weighted sum of the NTS-OU is again the NTS-OU process. This is an important feature in our quanto option pricing scheme which can be used to change to a one-dimensional NTS-OU process as follows. For the bivariate weighted sum, let $Z(t) = w_1X_1(t) + w_2X_2(t)$, then the mean and

the variance can be written as

$$\mathrm{E}[Z(t)] = w_1\mu_1 + w_2\mu_2,$$

$$\begin{aligned}\mathrm{Var}(Z(t)) = (w_1^2\sigma_1^2 + w_2^2\sigma_2^2)t + (w_1^2\beta_1^2 + w_2^2\beta_2^2 + 2w_1w_2\beta_1\beta_2)t\left(\frac{2-\alpha}{2\theta}\right) \\ + 2w_1w_2\sigma_1\sigma_2 E\left[\int_0^{\mathcal{T}(t)} \rho(s)ds\right].\end{aligned} \tag{3.4}$$

Hence, $Z(t)$ is the NTS-OU process with

$$Z(t) = \bar{\mu}t + \bar{\beta}(\mathcal{T}(t) - t) + \int_0^{\mathcal{T}(t)} \bar{\sigma}(s)dW(s),$$

where $\bar{\mu} = w_1\mu_1 + w_2\mu_2$, $\bar{\beta} = w_1\beta_1 + w_2\beta_2$, and

$$\bar{\sigma}(s) = \sqrt{w_1^2\sigma_1^2 + w_2^2\sigma_2^2 + 2w_1w_2\sigma_1\sigma_2\rho(s)}.$$

As we now have the description of the weighted sum of the two NTS-OU processes, the characteristic function needs to be derived in order to price the option with inverse Fourier transform. Let $\mathcal{F}_\rho(t)$ be the σ-algebra generated by $\{\rho(s)|0 \le s \le t\}$ then the characteristic function of $Z(t)$ is

given by

$$\begin{aligned}
\phi_{Z(t)}(u) &= E\left[E\left[E[\exp(iuZ(t))|\mathcal{F}_\rho(t)]|\mathcal{T}(t)\right]\right] \\
&= E\left[E\left[\exp\left(iu\left(\bar{\mu}t+\bar{\beta}(\mathcal{T}(t)-t)\right)-\frac{u^2}{2}\int_0^{\mathcal{T}(t)}\bar{\sigma}(s)^2ds\right)|\mathcal{T}(t)\right]\right] \\
&= E\left[E\left[\exp\left(iu\left(\bar{\mu}t+\bar{\beta}(\mathcal{T}(t)-t)\right)-\frac{u^2}{2}\left(w_1^2\sigma_1^2+w_2^2\sigma_2^2\right)\mathcal{T}(t)\right.\right.\right. \\
&\quad \left.\left.\left.-\frac{u^2}{2}2\int_0^{\mathcal{T}(t)}w_1w_2\sigma_1\sigma_2\rho(s)ds|\mathcal{T}(t)\right]\right] \\
&= \exp(iu(\bar{\mu}-\bar{\beta})t)E\left[\exp\left(i\left(u\bar{\beta}+\frac{iu^2}{2}\left(w_1^2\sigma_1^2+w_2^2\sigma_2^2\right)\right)\mathcal{T}(t)\right)\right] \\
&\quad E\left[E\left[\exp\left(-\frac{u^2}{2}2\int_0^{\mathcal{T}(t)}w_1w_2\sigma_1\sigma_2\rho(s)ds\right)|\mathcal{T}(t)\right]\right] \\
&= \exp(iu(\bar{\mu}-\bar{\beta})t)\phi_{\tau(t)}\left(u\bar{\beta}+\frac{iu^2}{2}\left(w_1^2\sigma_1^2+w_2^2\sigma_2^2\right)\right) \\
&\quad E\left[\exp\left(-u^2w_1w_2\sigma_1\sigma_2\int_0^{\mathcal{T}(t)}\rho(s)ds\right)\right].
\end{aligned}$$

For convenience, we define a process $(\mathcal{I}(\rho,t))_{t\geq 0}$ as $\mathcal{I}(\rho,t)=\int_0^t\rho(s)ds$ and let $\phi_{\mathcal{I}(\rho,t)}(u)$ be the characteristic function of $\mathcal{I}(\rho,t)$, then we can summarize as

$$\phi_{Z(t)}(u)=\exp(iu(\bar{\mu}-\bar{\beta})t)\phi_{\tau(t)}\left(u\bar{\beta}+\frac{iu^2}{2}\left(w_1^2\sigma_1^2+w_2^2\sigma_2^2\right)\right)E\left[\phi_{\mathcal{I}(\rho,\mathcal{T}(t))}(iu^2w_1w_2\sigma_1\sigma_2)\right]. \tag{3.5}$$

4 Quanto option pricing

We finally describe the derivation of the NTS-OU model where the complete specification of the modeling components, as well as the closed-form solution under the risk-neutral measure, are presented. We start this section by describing the previous quanto option pricing model: the NTS with constant correlation introduced by Kim *et al.* (2015). The NTS model is presented as a comparison model, which is also used in the numerical comparison section 5.

A quanto option is a European option where the payoff at expiry is converted at a pre-specified exchange rate to its corresponding currency. i.e. denoting F_{fix} to be the fixed exchange rate, $S(T)$ to be the underlying asset price in the specified foreign currency at expiry T, and K to be the strike, the quanto option payoff is,

$$F_{fix}(S(T) - K)^+.$$

Compared to a standard vanilla option, the quanto option introduces foreign exchange rate as an additional risk factor where the dependence structure of the underlying asset and the exchange rate is important for the valuation of quanto options.

Here, we introduce some notations to value quanto options. We denote r_d and r_f to be the interest rate for the domestic and foreign currency, respectively. Then, let $(S(t))_{t\geq 0}$ be the price process for the asset in foreign currency, $(V(t))_{t\geq 0}$ the price process of the asset in domestic currency, and $(F(t))_{t\geq 0}$ the exchange rate process of the foreign currency with respect to the domestic currency i.e. $S(t) = V(t)/F(t)$.

4.1 Black-Scholes quanto option pricing

Let's follow the notation and assume that $V(t)$ and $F(t)$ follows

$$V(t) = V(0)\exp(\mu_X t + \sigma_X W_X(t)),$$

and

$$F(t) = F(0)\exp(\mu_X t + \sigma_Y W_Y(t)),$$

where $(W_X(t))_{t\geq 0}$ and $(W_Y(t))_{t\geq 0}$ are Brownian motions with correlation being a constant ρ. To simplify the model, we assume that $W_Y(t) = \rho W_X(t) + \bar{\rho} + \bar{W}_Y(t)$, $\bar{\rho} = \sqrt{1-\rho^2}$ and that $W_X(t)$ and $\bar{W}_Y(t)$ are all independent to each other. By using Girsanov theorem to find a risk-neutral measure $\mathbb{Q}$, which makes $\exp(-r_d t)V(t)$ and $\exp(-(r_d - r_f)t)F(t)$ become martingales, we need to assume the risk of market price as the following

$$\lambda_1 = \frac{1}{\sigma_X}\left(\mu_X + \frac{1}{2}\sigma_X^2 - r_d\right),$$

$$\lambda_2 = \frac{\rho}{\sigma_X\bar{\rho}}\left(-\mu_X - \frac{1}{2}\sigma_X^2 + r_d\right) + \frac{1}{\sigma_Y\bar{\rho}}\left(\mu_Y + \frac{1}{2}\sigma_Y^2 - r_d + r_f\right).$$

Let's set $\bar{W}_X(t)$ and $\tilde{\bar{W}}_Y(t)$ to be

$$\tilde{W}_X(t) = \lambda_1 t + W_X(t),$$

and

$$\tilde{\bar{W}}_Y(t) = \lambda_2 t + W_Y(t),$$

respectively. Based on the theorem, there exists an equivalent measure $\mathbb{Q}$, such that $(\tilde{W}_X(t)_{t\geq 0})$, $(\tilde{\bar{W}}_Y(t)_{t\geq 0})$ are independent Brownian motions under

$\mathbb{Q}$. Now we have the followings:

$$V(t) = V(0)\exp\left(r_d t - \frac{\sigma_X^2}{2}t + \sigma_X \tilde{W}_X(t)\right),$$

$$F(t) = F(0)\exp\left((r_d - r_f)t - \frac{\sigma_Y^2}{2}t + \sigma_Y\rho\tilde{W}_X(t) + \sigma_Y\bar{\rho}\tilde{\tilde{W}}_Y(t)\right).$$

Since $S(t) = V(t)/F(t)$ we can easily derive its equation,

$$S(t) = S(0)\exp\left(r_f t - \frac{1}{2}(\sigma_X^2 - \sigma_Y^2)t + (\sigma_X - \sigma_Y\rho)\tilde{W}_X(t) - \sigma_Y\bar{\rho}\tilde{\tilde{W}}_Y(t)\right).$$

Now, let $\sigma^2 = \sigma_X^2 - 2\sigma_X\sigma_Y\rho + \sigma_Y^2$ and $(W(t))_{t\geq 0}$ be a Brownian motion independent to $(\tilde{W}_X(t))_{t\geq 0}$ and $(\tilde{\tilde{W}}_Y(t))_{t\geq 0}$ under risk-neutral measure $\mathbb{Q}$. The process then becomes $((\sigma_X - \sigma_Y\rho)\tilde{W}_X(t) - \sigma_Y\bar{\rho}\tilde{\tilde{W}}_Y(t))_{t\geq 0}$ the same as the process $(\sigma W(t))_{t\geq 0}$ in L^2,

$$\begin{aligned} S(t) &= S(0)\exp\left(r_f t - \frac{1}{2}(\sigma_X^2 - \sigma_Y^2)t + (t)\right) \\ &= S(0)\exp\left(r_f t + (\sigma_Y^2 - \sigma_X\sigma_Y\rho)t - \frac{\sigma^2}{2}t + \sigma W(t)\right). \end{aligned}$$

Let's recall that the payoff function of a quanto option is $F_{fix}(S(T) - K)^+$, where F_{fix} is a given exchange rate in the contract. Let $(\mathcal{F}_t)_{t\geq 0}$ be the filtration. By the Black-Scholes formula, the price of a quanto call option, c, at time t is

$$\begin{aligned} c &= e^{-r_d(T-t)}E_{\mathbb{Q}}[F_{fix}(S(T) - K)^+|\mathcal{F}_t] \\ &= F_{fix}\left(e^{(r_f - r_d + \sigma_Y^{\mathbb{Q}} - \rho\sigma_X\sigma_Y)(T-t)}S(t)N(d_1) - e^{-r_d(T-t)}KN(d_2)\right), \end{aligned}$$

where

$$d_1 = \frac{(r_f + \sigma_Y^2 - \rho\sigma_X\sigma_Y)(T-t) + \log(S(t)/K)}{\sigma\sqrt{T-t}},$$

$$d_2 = d_1 - \sigma\sqrt{T-t},$$

and $N(\cdot)$ is a cumulative standard normal distribution function. By following the same process the quanto put option price becomes

$$\begin{aligned} p &= \mathrm{e}^{-r_d(T-t)} E_{\mathbb{Q}}[F_{fix}(K - S(T))^+ | \mathcal{F}_t] \\ &= F_{fix}\left(\mathrm{e}^{-r_d(T-t)}KN(-d_2) - \mathrm{e}^{(r_f - r_d + \sigma_Y^2 - \rho\sigma_X\sigma_Y)(T-t)}S(t)N(-d_1)\right). \end{aligned}$$

4.2 NTS quanto option pricing with constant correlation

We recap the pricing model for quanto option with the NTS process, assuming constant correlation. We present the derived analytical formula so that it can be compared to our approach in the next section (4.3) with stochastic correlation. For the underlying processes, we assume that $(V(t))_{t\geq 0}$ and $(F(t))_{t\geq 0}$ are given by

$$\begin{aligned} V(t) &= V(0)\exp\left(\mu_X t + X(t)\right), \\ F(t) &= F(0)\exp\left(\mu_Y t + Y(t)\right), \end{aligned} \tag{4.1}$$

where the NTS process $X(t)$ and $Y(t)$ are following the bivariate processes under physical measure $\mathbb{P}$,

$$\begin{bmatrix} X \\ Y \end{bmatrix} \sim NTS_2\left[\alpha, \theta, \begin{pmatrix} 0 \\ 0 \end{pmatrix}, \begin{pmatrix} \beta_X \\ \beta_Y \end{pmatrix}, \begin{pmatrix} \sigma_X \\ \sigma_Y \end{pmatrix}, \begin{pmatrix} 1 & \rho \\ \rho & 1 \end{pmatrix}\right].$$

The goal is to convert these processes into risk-neutral measure and eventually calculate the characteristic function under risk-neutral measure for the asset price denoted in foreign currency, i.e. $S(t)$ in our notation. We do so by applying the Theorem 3.1 (Girsanov). The detailed derivation of risk-neutral measure can be seen in reference Kim *et al.* (2015) where we present a summary of the approach and its results here. We derive it with the condition that discounted price processes for $\hat{V}(t) = e^{-r_d t}V(t)$ and $\hat{F}(t) = e^{-(r_d+r_f)t}F(t)$ are martingales under $\mathbb{Q}$-measure i.e.:

$$E_{\mathbb{Q}}[\hat{V}(t)] = V(0),$$

$$E_{\mathbb{Q}}[\hat{F}(t)] = F(0),$$

these conditions lead to λ^* satisfying

$$\lambda_X^* < \theta - \beta_X - \frac{\sigma_X^2}{2} \quad and \quad \lambda_Y^* < \theta - \beta_Y - \frac{\sigma_Y^2}{2},$$

$$\mu_X - r_d + w_X(\lambda_X^*) = 0 \; and \; \mu_Y - r_d + r_f + w_Y(\lambda_Y^*) = 0,$$

where $w_X(\lambda_X^*) = logE_{\mathbb{Q}_{\lambda^*}}[e^{X(1)}]$ and $w_Y(\lambda_Y^*) = logE_{\mathbb{Q}_{\lambda^*}}[e^{Y(1)}]$. Then there exist an equivalent martingale measure $\mathbb{Q}$ under which

$$V(t) = V(0)\exp((r_d - w_X(\lambda_X^*)t + X(t)),$$

$$F(t) = F(0)\exp((r_d - r_f - w_Y(\lambda_Y^*)t + Y(t)),$$

for $t \geq 0$ which subsequently means

$$S(t) = S(0)\exp((r_f - w(\lambda_X^*) + w(\lambda_Y^*))t + Z(t)),$$

where $Z(t) = X(t) - Y(t)$. By proposition 1, $Z(t)$ follows the NTS process with the following parameters, i.e, $Z \sim NTS_1(\alpha, \theta, \gamma_Z, \beta_Z, \sigma_{Z,1})$ where the parameters are $\gamma_Z = \lambda_X^* - \lambda_Y^*$, $\beta_Z = \beta_X + \lambda_z^* - \beta_Y - \lambda_Y^*$ and finally $\sigma_Z = \sqrt{(\sigma_X^2 + \sigma_Y^2 - 2\sigma_X\sigma_Y\rho)}$. With these parameters following one-dimensional NTS, we can get the characteristic function directly from equation 2.10:

$$\phi_{Z(t)}(u) = \exp\Bigg(-(\beta_X - \beta_Y)iut - \frac{2t\theta^{1-\frac{\alpha}{2}}}{\alpha}\Bigg(\Bigg(\theta - i(\beta_X + \lambda_X^* - \beta_Y - \lambda_Y^*)u + \frac{u^2}{2}(\sigma_X^2 + \sigma_Y^2 - 2\sigma_X\sigma_Y\rho)\Bigg)^{\frac{\alpha}{2}} - \theta^{\frac{\alpha}{2}}\Bigg)\Bigg).$$

With the derived characteristic function, we can price the quanto option with the use of general European option pricing (Theorem 4.1): Let $T \geq 0$ then the quanto call option price is

$$\begin{aligned} C_t^{Quanto}(K,T) &= \exp(-r_d(T-t))E^{\mathbb{Q}}\left[F_{fix}(S(T)-K)^+|\mathcal{F}_t\right] \\ &= \frac{e^{-r_d(T-t)F_{fix}K^{1+\xi}}}{2\pi S(t)\xi e^{\xi(r_f - w_X(\lambda_X^*) + w_Y(\lambda_Y^*))(T-t)}} G(\frac{1}{2\pi} log(\frac{K}{S(t)})), \end{aligned} \tag{4.2}$$

where $\mathcal{F}_t$ is a filtration and

$$G(x) = \int e^{-2\pi iux} \frac{e^{iu(r_f - w_X(\lambda_X^*) + w_Y(\lambda_Y^*))(T-t)}}{(iu - \xi - 1)(iu - \xi)} E[e^{(iu-\xi)Z(T-t)}]du,$$

with $Z = X - Y$ and $\xi \in \mathbb{R}$.

4.3 NTS quanto option pricing with stochastic correlation

We follow the notation and the framework setup in the previous section 4.2. Let's assume (4.1) for the underlying dynamics of the quanto option and model them via bivariate NTS processes with stochastic correlations.

$$(X,Y) \sim \text{NTS}_{OU}\left(\alpha, \theta, \begin{pmatrix} 0 \\ 0 \end{pmatrix}, \begin{pmatrix} \beta_X \\ \beta_Y \end{pmatrix}, \begin{pmatrix} \sigma_X \\ \sigma_Y \end{pmatrix}, \begin{pmatrix} 1 & \rho(t) \\ \rho(t) & 1 \end{pmatrix}_{t\geq 0}\right),$$

with a bounded stochastic process $\rho = (\rho(t))_{t\geq 0}$ under the physical measure $\mathbb{P}$. Similarly, as the previous model discussed in section 4.2, the next step is to find the risk-neutral measure for pricing. Together with, $\lambda^* = (\lambda_X^*, \lambda_Y^*)^\intercal$, and by Proposition 2, we can find its unique equivalent martingale measure $\mathbb{Q}_{\lambda^*}$,

$$(X,Y) \sim \text{NTS}_{OU}\left(\alpha, \theta, \begin{pmatrix} \lambda_X^* \\ \lambda_Y^* \end{pmatrix}, \begin{pmatrix} \beta_X + \lambda_X^* \\ \beta_Y + \lambda_Y^* \end{pmatrix}, \begin{pmatrix} \sigma_X \\ \sigma_Y \end{pmatrix}, \begin{pmatrix} 1 & \rho(t) \\ \rho(t) & 1 \end{pmatrix}_{t\geq 0}\right).$$

We calculate the risk-neutral measure as follows. With the changed measure, the discounted price processes becomes martingale, i.e. $E_{\mathbb{Q}_{\lambda^*}}\left[\tilde{V}(t)\right] = V(0)$ and $E_{\mathbb{Q}_{\lambda^*}}\left[\tilde{F}(t)\right] = F(0)$ where $\tilde{V}(t) = e^{-r_d t}V(t)$ and $\tilde{F}(t) = e^{(-r_d+r_f)t}F(t)$. This is equivalent to $E_{\mathbb{Q}_{\lambda^*}}\left[e^{X(t)}\right] = e^{-(\mu_X - r_d)t}$, and $E_{\mathbb{Q}_{\lambda^*}}\left[e^{Y(t)}\right] = e^{-(\mu_Y - r_d + r_f)t}$. Hence, this implies λ^* has to satisfy the following two conditions:

Condition 1: $\lambda_X^* < \theta - \beta_X - \frac{\sigma_X^2}{2}$ and $\lambda_Y^* < \theta - \beta_Y - \frac{\sigma_Y^2}{2}$ so that $E_{\mathbb{Q}_{\lambda^*}}\left[e^{X(t)}\right]$ and $E_{\mathbb{Q}_{\lambda^*}}\left[e^{Y(t)}\right]$ exist.

Condition 2: $\mu_X - r_d + w(\lambda_X^*) = 0$ and $\mu_Y - r_d + r_f + w(\lambda_Y^*) = 0$, where

$$w(\lambda_X^*) = \log E_{\mathbb{Q}_{\lambda^*}}\left[e^{X(1)}\right] = -\beta_X - \frac{2\theta^{1-\frac{\alpha}{2}}}{\alpha}\left(\left(\theta - \beta_X - \lambda_X^* - \frac{\sigma_X^2}{2}\right)^{\frac{\alpha}{2}} - \theta^{\frac{\alpha}{2}}\right),$$

$$w(\lambda_Y^*) = \log E_{\mathbb{Q}_{\lambda^*}}\left[e^{Y(1)}\right] = -\beta_Y - \frac{2\theta^{1-\frac{\alpha}{2}}}{\alpha}\left(\left(\theta - \beta_Y - \lambda_Y^* - \frac{\sigma_Y^2}{2}\right)^{\frac{\alpha}{2}} - \theta^{\frac{\alpha}{2}}\right).$$

Since we have $\mu_X = r_d - w(\lambda_X^*)$ and $\mu_Y = r_d - r_f - w(\lambda_Y^*)$, dynamics under the risk-neutral measure becomes the following:

$$V(t) = V(0)\exp\left((r_d - w(\lambda_X^*))t + X(t)\right),$$
$$F(t) = F(0)\exp\left((r_d - r_f - w(\lambda_Y^*))t + Y(t)\right).$$

As now we found the dynamics of $V(t)$ and $F(t)$ under the new risk-neutral measure, the asset price in foreign currency $S(t)$ can be formulated as below.

$$S(t) = \frac{V(t)}{F(t)} = S(0)\exp\left(\left(r_f - w(\lambda_X^*) + w(\lambda_Y^*)\right)t + Z(t)\right), \tag{4.3}$$

where $Z(t) = X(t) - Y(t)$, with measure $\mathbb{Q}_{\lambda^*}$. We apply the Proposition 1 again, where we now have the weights of $w = (1, -1)^\intercal$, for $Z = (Z(t))_{t\geq 0}$:

$$Z(t) = \lambda_Z t + \beta_Z(\mathcal{T}(t) - t) + \int_0^{\mathcal{T}(t)} \sigma_Z(s)dW(s), \quad t \geq 0.$$

Here, the parameters have changed as follows; $\lambda_Z = \lambda_X^* - \lambda_Y^*$, $\beta_Z = \beta_X + \lambda_X^* - \beta_Y - \lambda_Y^*$, and $\sigma_Z(t) = \sqrt{\sigma_X^2 + \sigma_Y^2 - 2\sigma_X\sigma_Y\rho(t)}$. $(W(t))_{t\geq 0}$ is an one-dimensional Brownian motion independent of ρ and $\mathcal{T}$. Now we can get the characteristic function of $Z(t)$ with the given parameters and equation

(3.5) which is

$$\phi_{Z(t)}(u) = \exp(iu(\lambda_Z - \beta_Z)t)\phi_{\tau(t)}\left(u\beta_Z + \frac{iu^2}{2}\left(\sigma_X^2 + \sigma_Y^2\right)\right) E\left[\phi_{\mathcal{I}(\rho,\mathcal{T}(t))}(-iu^2\sigma_X\sigma_Y)\right]. \tag{4.4}$$

With the dynamics of the price process $S(t)$ in (4.3) and the characteristic function of $Z(t)$, we find the general European option pricing formula given in Lewis (2001) to price the quanto option. Then, we utilize an inverse Fourier transform to calculate the price numerically.

Theorem 4.1. *Let $h(x)$ be a payoff function of a given European option with $x = \log S(T)$ and $\hat{h}(\xi) = \int_{-\infty}^{\infty} e^{-i\xi x}h(x)dx$. Suppose $\hat{h}(\xi)$ is defined for all $\xi \in R_h = \{z \in \mathbb{C} : \mathrm{Im}(z) \in I_h\}$, for some open interval I_h. The driving process $(U(T))_{t\geq 0}$, with $U(t) = \ln S(t)$, is a Lévy process, such that a characteristic function $\phi_{U(T-t)}(u)$ of $U(T-t)$ is defined for all $\xi \in R_\phi = \{z \in \mathbb{C} : \mathrm{Im}(z) \in I_\phi\}$, for some open interval I_ϕ. Then, the European option price $C(t)$ at time t is determined by*

$$C(t) = \frac{e^{-r_d(T-t)}}{2\pi}\int_{-\infty}^{\infty}(S(t))^{i(u+i\zeta)}\phi_{U(T-t)}(u+i\zeta)\hat{h}(u+i\zeta)du,\ \zeta \in I_h \cap I_\phi. \tag{4.5}$$

We layout the components of the above equation (4.5). Firstly, the payoff function of the quanto option is $F_{fix}(S(T)-K)^+$, thus we rewrite it to be

$$h(x) = F_{fix}(e^x - K)^+ \text{ and } \hat{h}(\xi) = -F_{fix}K^{1-i\xi}/\xi(\xi+i). \tag{4.6}$$

$\hat{h}(\xi)$ is well defined for $\xi \in \{z \in \mathbb{C} : \mathrm{Im}(z) \in I_h = (-\infty, -1)\}$. In order to get the characteristic function of $U(T-t)$, i.e. $\phi_{U(T-t)}$, by (4.3) and (4.4),

we have

$$U(t) = \bar{\mu}_Z t + \beta_Z(\mathcal{T}(t) - t) + \int_0^{\mathcal{T}(t)} \sigma_Z(s) dW(s), \quad t \geq 0,$$

where $\bar{\mu}_Z = r_f - w(\lambda_X^*) + w(\lambda_Y^*) + \lambda_X^* - \lambda_Y^*$. Since

$$U(T-t) = \left(r_f - w(\lambda_X^*) + w(\lambda_Y^*)\right)(T-t) + Z(T-t), \tag{4.7}$$

the characteristic function of $U(T-t)$ becomes

$$\phi_{U(T-t)}(\xi) = e^{i\xi(r_f - w(\lambda_X^*) + w(\lambda_Y^*))(T-t)} \phi_{Z(T-t)}(\xi). \tag{4.8}$$

Note that both functions $\phi_{U(T-t)}(\xi)$ and $\phi_{Z(T-t)}(\xi)$ are well defined for $\xi \in \{z \in \mathbb{C}\colon\ \mathrm{Im}(z) \in I_{\phi_Z}\}$ with

$$I_{\phi_Z} = \left[-\frac{1}{\sigma_Z^2}\left(\beta_Z + \sqrt{\beta_Z^2 + 2\sigma_Z^2\theta}\right), \frac{1}{\sigma_Z^2}\left(\sqrt{\beta_Z^2 + 2\sigma_Z^2\theta} - \beta_Z\right)\right].$$

By Theorem 4.1, for a given strike K and maturity T, the European quanto call price is

$$C_{K,T}(t) = \frac{e^{-r_d(T-t)}}{2\pi} \int_{-\infty}^{\infty} (S(t))^{i(u+i\zeta)} \frac{F_{fix} K^{1-i(u+i\zeta)} \phi_{U(T-t)}(u+i\zeta)}{(-1)(u+i\zeta)(u+i(\zeta+1))} du, \tag{4.9}$$

with $\zeta \in \left[-\frac{1}{\sigma_Z^2}\left(\beta_Z + \sqrt{\beta_Z^2 + 2\sigma_Z^2\theta}\right), -1\right]$, given $\frac{1}{\sigma_Z^2}\left(\beta_Z + \sqrt{\beta_Z^2 + 2\sigma_Z^2\theta}\right) > 1$.

Following the same process, we can derive a pricing formula for a European quanto put option for $\zeta \in \left[0, \frac{1}{\sigma_Z^2}\left(\sqrt{\beta_Z^2 + 2\sigma_Z^2\theta} - \beta_Z\right)\right]$. Also, the integral in (4.9) can be calculated via FFT to effectively calculate the price. We show the calculation process in the empirical section.

As the pricing formula based on the bivariate NTS process with the stochastic correlation is given, we specify the OU process that we choose for the stochastic correlation. More specifically, this will change the quanto option pricing formula by determining $E\left[\phi_{\mathcal{I}(\rho,\mathcal{T}(t))}(-iu^2\sigma_X\sigma_Y)\right]$ in the the equation (4.4) and eventually $\phi_{U(T-t)}$ in the final pricing formula (4.9).

Let's recall that we defined $(\mathcal{I}(\rho,t))_{t\geq 0}$ as $\mathcal{I}(\rho,t) = \int_0^t \rho(s)ds$. Now, our model of choice for the correlation $(\rho(t))_{t\geq 0}$ over time is the Ornstein-Uhlenbeck (OU) Process as follows:

$$d\rho(t) = -\kappa_{OU}\rho(t)dt + \sigma_{OU}dW(t).$$

The solution of the above OU process is

$$\rho(t) = \rho(0)e^{-\kappa_{OU}t} + \sigma_{OU}\int_0^t e^{-\kappa_{OU}(t-s)}dW(s). \tag{4.10}$$

Moreover, $\mathcal{I}(\rho,t) = \int_0^t \rho(s)ds$ follows the normal distribution with the mean

$$E\left(\int_0^t \rho(s)ds\right) = \rho(0)D(t),$$

and the variance

$$\text{var}\left(\int_0^t \rho(s)ds\right) = \frac{\sigma_{OU}^2}{\kappa_{OU}^2}\left(t - D(t) - \frac{\kappa_{OU}}{2}(D(t))^2\right),$$

where

$$D(t) = \frac{1-e^{-\kappa_{OU}t}}{\kappa_{OU}}.$$

Finally, the characteristic function of $\mathcal{I}(\rho,t)$ is equal to

$$\begin{aligned}\phi_{\mathcal{I}(\rho,t)}(u) &:= E\left[\exp\left(iu\int_0^t \rho(s)ds\right)\right] \\ &= \exp\left(iuE\left(\int_0^t \rho(s)ds\right) - \frac{u^2}{2}\mathrm{var}\left(\int_0^t \rho(s)ds\right)\right) \\ &= \exp\left(iu\rho(0)D(t) - \frac{u^2\sigma_{OU}^2}{2\kappa_{OU}^2}\left(t - D(t) - \frac{\kappa_{OU}}{2}(D(t))^2\right)\right).\end{aligned} \tag{4.11}$$

By plugging (4.11) into equation (4.4), we can get the $\phi_{U(t)}$ which in turn completes the analytical pricing formula in equation (4.9).

5 Empirical application

The main purpose of this section is to demonstrate that the NTS-OU enhances performance in pricing quanto options. To analyze the performance of our model, we conduct experiments on the two quanto option contracts and compare the NTS-OU performance with the BS model and the NTS model with constant correlation. The two quanto contracts are the following: a contract on the S&P 500 index option with the EUR-USD exchange rate, and a contract on the DJIA option with the Bitcoin-USD exchange rate.

The first quanto option is designed to evaluate the model performance when the correlation is mostly staying positive due to macroeconomic causality. On the other hand, the latter quanto example is to assess the performance in a case where the historical correlation often fluctuates around zero

and spikes when the market in distress. By conducting the calibration in two different market regimes, we show that the performance of the NTS-OU model works well in general cases.

We first present the statistical summary of the underlying dynamics. The return distribution of each underlying asset and the historical rolling correlation between the underlying assets are analyzed by the marginal distribution plots, the Quantile-Quantile (Q-Q) plots, and the Kolmogorov-Smirnov (KS) test. At this level, we show that the NTS is the best-fitted process for the empirical data, and the OU process is a proper assumption to describe the stochastic correlation.

Then, we calibrate risk-neutral parameters under the BS model and NTS model, and the NTS-OU model for ten trading days in 2019. The goodness-of-fit test was performed on the calibrated parameters: average absolute error (AAE), the average absolute error as a percentage of the mean price (APE), and the root mean square error (RMSE) are reported in favor of the NTS-OU model. A term-structure on one specific trading date with multiple expiries is provided as well.

In our notation, $V(t)$ is the dollar valued price process of SPX (or DJIA), $S(t)$ is the EUR (or BTC) valued price process and $F(x)$ is the exchange rate process.

5.1 A quanto option on the S&P 500 index and the EUR-USD

In this experiment, we investigate the quanto option of the S&P 500 index and the EUR-USD exchange rate as underlying assets. We use data over a period from January 2015 to June 2020. For parameter calibration,

data of ten trading dates in August 2019 is used.

5.1.1 In sample test: fitting the S&P 500 and the EUR-USD

The basic statistical summary of the daily log-return distribution is shown in Table 1 on the aforementioned timeframe. We note that the high kurtosis, 20.8514 for S&P 500 and 5.6368 for EUR-USD, are well over 3 (the normal distribution case) and it indicates a strong leptokurtic nature for both underlying assets. The normal distribution is not capable of explaining such high kurtosis, so the assumption of the normal distribution in the BS model is clearly rejected on the empirical grounds.

	S&P 500	EUR-USD
Mean	3.1688×10^{-04}	-4.9179×10^{-05}
Standard Deviation	0.0125	0.0053
Skewness	-0.9548	-0.0394
Kurtosis	20.8514	5.6368
$Q_{.01}$	-0.1034	-0.0269
$Q_{.05}$	-0.0482	-0.0173
$Q_{.1}$	-0.0342	-0.0142
$Q_{.5}$	-0.0178	-0.0081
$Q_{.95}$	0.0156	0.0086
$Q_{.99}$	0.0309	0.0139
$Q_{.995}$	0.0470	0.0155
$Q_{.999}$	0.0889	0.0226

Table 1: Summary statistics for daily log-returns of the S&P 500 and the EUR-USD exchange rate from January 2015 to June 2020. The high kurtosis well exceeding over 3 (the normal distribution case) shows that the empirical density is substantially leptokurtotic.

The skewness and the heavy tails of the underlying assets can be more clearly observed in the density distribution and the Q-Q plots as displayed in Figure 2. In line with the previous summary statistics, there is an evident contrast between the NTS distribution and the normal distribution.

The NTS distribution traces the empirical return distribution closely with its flexible shape, whereas the fixed shape parameters of the normal distribution don't capture it well. The Q-Q plot also displays the poor fits of the normal distribution in the both tails area in particular, whereas the NTS distribution displays a better fit in all areas.

5.1.2 The Kolmogorov Smirnov (KS) test

The Kolmogorov-Smirnov (KS) test is used to quantify the fitted quality of all three candidate distributions - the NTS distribution, the Student's t distribution, and the normal distribution. This particular goodness-of-fit property is defined as

$$KS = \sup_x |\hat{F}(x) - F(x)|,$$

where $\hat{F}(x)$ is the real sample distribution and $F(x)$ is the estimated distribution by the hypothesized distribution.

This non-parametric test is known to have a shortcoming of rejecting the null hypothesis when extremely large data is used. Hence, we controlled the number of observations to be 1382, from January 2015 to June 2020. The KS statistics and its corresponding p-value is presented in Table 2. The null hypothesis that the sample is drawn from the reference distribution is soundly rejected for the normal distribution at the significance level of 5%. For the Student's t and the NTS distributions, the null hypothesis is not rejected where the NTS shows a higher p-value than the Student's t in both the S&P 500 and the EUR-USD, suggesting the best fits for all candidate distributions.

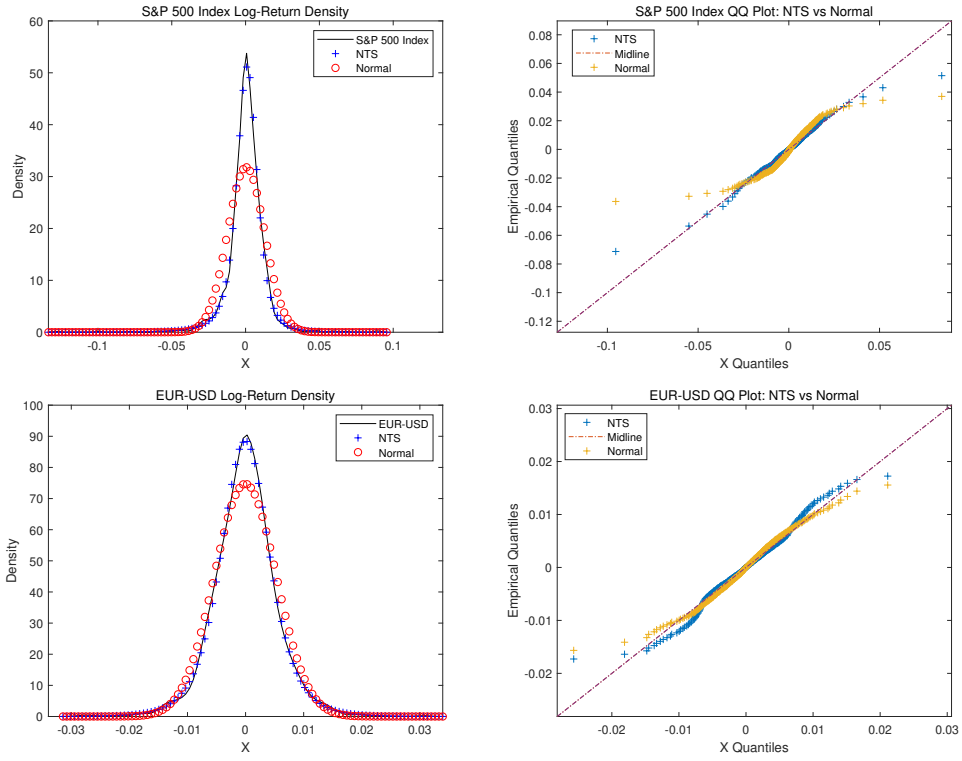

Figure 2: The log-return density distribution (left) and the Q-Q plot (right) for both the S&P 500 index and the EUR-USD. The NTS distribution and the normal distribution are fitted. The empirical density shows the leptokurtic nature, but the Normal distribution cannot capture the peakedness of the density distribution for both underlying assets. In the Q-Q plots, the normal distribution fits well around the center whereas the fit becomes poorer in the tails. The NTS distribution shows a better fit on all plots.

	S&P 500		EUR-USD	
Distribution	KS Statistics	*p-value*	KS Statistics	*p-value*
Normal	0.1056	0.0001	0.0469	0.0034
Student's t	0.023	0.422	0.0169	0.7993
NTS	0.0072	0.9997	0.0056	0.9921

Table 2: p-values of the KS test for three candidate distribution in the S$P 500 and the EUR-USD at 5% of the significance level. The NTS strongly beats the other candidates the normal and the Student's t.

5.1.3 Stochastic Correlation between the S&P 500 and the EUR-USD

The main objective of the NTS-OU model is to include the stochastic correlation feature in the quanto option pricing. Observing the stochastic correlation presented in the historical data gives us additional confidence in modeling this feature.

Figure 3 shows the moving correlation with three different windows: 30 days, 60 days and 90 days. It is evident that the correlation between the S&P 500 and the EUR-USD is varying significantly over time. As the observation of Figure 3 confirms, assuming the correlation between assets as a constant is erroneous and it may return the bad price estimates when the market is in volatile times particularly. In fact, it is a well-documented fact that (1) the correlation on the multivariate financial assets is time-varying (see Patton (2006)), and (2) the correlation is more unstable than the volatility (see Ma (2009)). In the following calibration test, we will show that the NTS-OU model considering the stochastic correlation returns the best estimates than the previous models.

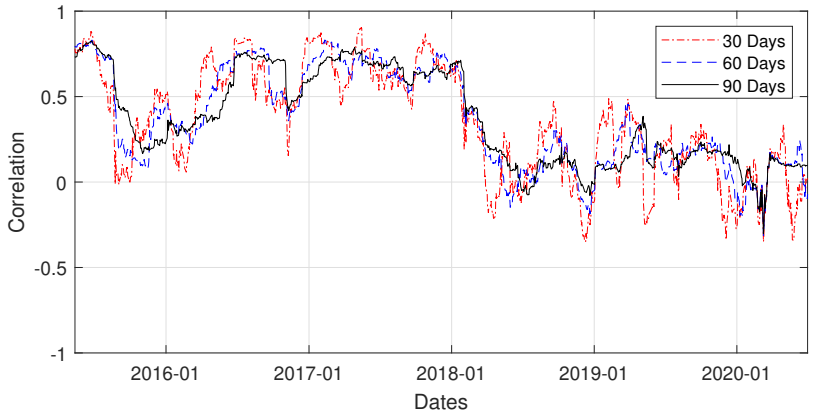

Figure 3: Illustration of the historical rolling correlation between the S&P 500 and the EUR-USD returns over the period of January 2015 and June 2020.

5.1.4 Calibration to the quanto option

Given the strong empirical support for the NTS-OU model as presented in the previous sections, we now expect to see an improved estimate of the quanto option price. To show this enhanced performance of the NTS-OU, we conduct the parameter calibration for all three models: the NTS-OU, the BS, and the NTS with constant correlation.

The assessment has the following steps. Since there are limited available traded quanto option price data, we first proxy the data. Recall that the full quanto option price is calculated with $e^{-r_d(T-t)}F_{fix}E_Q[(S(T)-K)^+|\mathcal{F}_t]$ and $e^{-r_d(T-t)}F_{fix}E_Q[(K-S(T))^+|\mathcal{F}_t]$ for call and put, respectively. The parts $E_Q[(S(T)-K)^+|\mathcal{F}_t]$ and $E_Q[(K-S(T))^+|\mathcal{F}_t]$ are replaced with the market price of SPX call and put options. After the previous data proxy step, we calibrate risk-neutral parameters to both put and call option price data on 10 selected trading dates. This is conducted by the least-squares minimization of the distance between data and theoretical quanto prices

from the models. Note that the calibration is performed on a set of option prices with all different strike K on a given trading day. The expiry date is chosen to be the closest available date to three months from the trading date.

The estimated prices of both call and put quanto options on August 5, 2019 are illustrated in Figure 4 as a sample. The price from all three comparison models and the proxy market data are plotted together against the different strikes. It is visually evident that the NTS-OU is the most flexible model that display the closest to the proxy-quanto option price for a wide range of strike prices. This is because NTS-OU is the only model that is capable of capturing the heavy tails, the skewness as well as the stochastic correlation.

The calibrated parameters for all the three models are summarized in Table 3 and its goodness-of-fit test result is presented in 4. For the BS model, we estimate σ_1, σ_2, and ρ^2, and for the NTS, we calibrate α, θ, λ_Z, β_Z, σ_1, σ_2, ρ and μ_Z where $Z(t) = X(t) - Y(t)$ in our notation[3]. The NTS-OU, as described previously, the OU parameters θ_{OU}, σ_{OU}, κ_{OU}[4]are added to the NTS parameter list. Note that, as we remarked before, we fixed the long-term mean θ_{OU} to be zero for the calibration stability.

At a glance, we find that the OU parameters are significantly different from zero, indicating that added flexibility in the correlation dynamics enables the better-fitted option price in the risk-neutral space. Also, all of the

[2] σ_1 is the standard deviations for the S&P 500 index, σ_2 is the standard deviations for the exchange rate and ρ is the correlation between two underlyg assets.

[3] α represent fat-tailedness and peakedness, and jump intensity. θ means the 'tempering' parameter for the subordinator. λ is the drift term. β is the skewness parameter, and σ presents the scale parameter. ρ means the dependency between the underlying dynamics.

[4] θ_{OU} is the mean of the fundamental process, σ_{OU} is the volatility, and κ_{OU} is the speed to reverts towards the mean.

calibrated α is far below 2 which means the substantial fat-tailedness and the skewness appeared on this quanto option dynamics.

Date	Model	α	θ	λ_Z	β_Z	σ_1	σ_2	μ_Z	ρ_0	σ_{OU}	κ_{OU}
05-Aug-2019	BS					0.7762	0.6258		0.9965		
	NTS	0.0001	1.9557	-0.0052	0.1790	0.1502	0.0906	0.0005			
	NTS-OU	0.2549	2.1592	0.0018	0.3702	0.0735	0.0735	0.0002	0.2416	2.6914	13.4179
08-Aug-2019	BS					0.7434	0.6113		1.0000		
	NTS	1.3372	0.1143	0.0052	0.0810	0.1508	0.0908	-0.0005			
	NTS-OU	1.3198	1.5552	-0.0173	0.3664	0.1268	0.0379	0.0018	0.9999	0.0000	0.6678
13-Aug-2019	BS					0.7313	0.5936		1.0000		
	NTS	0.0001	1.6484	-0.0191	0.1422	0.1186	0.0756	-0.0029			
	NTS-OU	0.5193	1.4461	-0.0104	0.2750	0.0668	0.0669	0.0010	0.0423	3.7562	15.0887
15-Aug-2019	BS					0.7185	0.5601		1.0000		
	NTS	0.0001	2.7481	-0.0070	0.1561	0.1512	0.09309	0.0008			
	NTS-OU	1.3978	3.33E-05	-0.0045	0.5329	0.0010	0.1088	0.0004	-0.2119	-0.2855	2.3407
21-Aug-2019	BS					0.7390	0.6099		0.9993		
	NTS	1.3866	0.0986	0.0054	0.0660	0.1519	0.0905	-0.0005			
	NTS-OU	1.0706	4.6120	-0.0095	0.4499	0.0760	0.0695	0.0010	0.7028	3.3230	9.3295
23-Aug-2019	BS					0.6835	0.5340		0.9984		
	NTS	0.0001	1.9362	-0.0198	0.1310	0.1524	0.0905	0.0015			
	NTS-OU	1.2044	2.4331	-0.0209	0.5734	0.0010	0.0010	0.0016	0.0671	3.2780	14.1898
26-Aug-2019	BS					0.6744	0.5274		0.9998		
	NTS	0.0001	1.4247	-0.0156	0.1117	0.1524	0.0906	0.0016			
	NTS-OU	1.2211	1.6345	-0.0145	0.3698	0.1235	0.1235	0.0014	0.9999	0.0000	4.5280
27-Aug-2019	BS					0.7191	0.5702		0.9986		
	NTS	0.0001	1.5525	-0.0100	0.1321	0.1524	0.0906	0.0020			
	NTS-OU	0.2466	2.0911	-0.0044	0.3306	0.0709	0.0713	0.0014	0.2520	2.8400	14.1381
29-Aug-2019	BS					0.7119	0.5703		1.0000		
	NTS	0.0001	1.8116	-0.0089	0.1499	0.1336	0.0516	0.0071			
	NTS-OU	1.0114	1.3320	-0.0074	0.2917	0.1139	0.1138	0.0067	0.9999	0.0000	6.3784
30-Aug-2019	BS					0.7391	0.5966		1.0000		
	NTS	0.0001	1.8816	0.0020	0.1631	0.1186	0.0753	0.0126			
	NTS-OU	1.0114	1.3320	-0.0074	0.2917	0.1139	0.1138	0.0067	0.9999	0.0000	6.3784

Table 3: Calibrated risk-neutral parameters under the BS, the NTS and the NTS-OU models for the S&P 500 and the EUR-USD quanto option. Note that the estimated α is well below 2 which implies the heavy tails and skewness in this quanto option dynamics.

To evaluate the performance of the three comparison models more specifically, we calculated the three measures of the goodness-of-fit test: AAE, APE, and RMSE [5]. For all selected trading dates, the NTS-OU model consistently reports the lowest value for all three measures with only a few exceptions. On the other hand, the BS model underperforms for all measures and trading days. The order of performance of the three models

[5]The error estimators follows:
AAE(Average Absolute Error) $= \sum_{j=1}^{N} \frac{|\hat{P}_j - P_j|}{N}$
APE(Average Prediction Error) $= \frac{\sum_{j=1}^{N} |\hat{P}_j - P_j|/N}{\sum_{j=1}^{N} |\hat{P}_j|/N}$
$RMSE$(Root Mean - Square Error) $= \sqrt{\sum_{j=1}^{N} \frac{(\hat{P}_j - P_j)^2}{N}}$

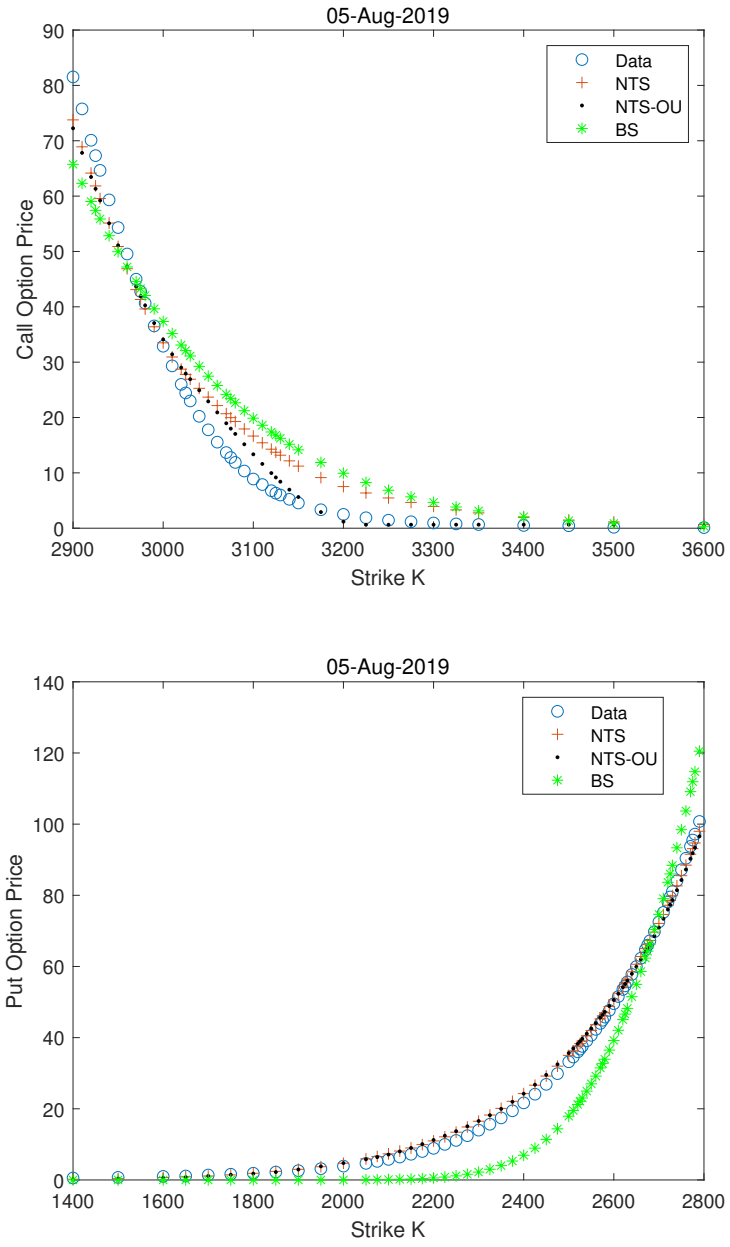

Figure 4: Comparing the estimated prices for the quanto option of the SPX and EUR-USD on August 5, 2019. The NTS-OU is the best performer, followed by the NTS and then the BS.

is evident based on the goodness-of-fit measures: NTS-OU, NTS, and BS. Having discussed the goodness-of-fit test result, we conclude that the adding the OU and NTS parameters to the BS model significantly contribute to the accurate pricing estimation as the parameters reflect the empirical evidence.

The goodness-of-fit test result of the risk-neutral parameter calibration have another important implication on the risk-neutral world. As the added OU parameters enhance the model performance, we can infer that the stochastic correlation property exists in the risk-neutral world.

Now we offer the term structure in which model performance is estimated with different expiries for one trading day. The selected trade date is Aug 15th, 2019, and 30, 60, 90 days are considered as a time-to-maturity. As can be seen in Figure 5, the NTS-OU has more flexibility to fit the asymmetric shape of the option prices across multiple expirations. Based on the RMSE, we can confirm again that the BS model (18.9876) clearly underperforms for all strike prices. The NTS model (10.173) is the next whereas the NTS-OU (6.4119) provides the best fitting capability.

5.2 A quanto option on the DJIA and the BTC-USD

Bitcoin is a new type of financial instrument that emerged as a cryptocurrency in 2008 and gained popularity over recent years. The spirit behind Bitcoin is creating a new decentralized currency that is independent of any central banks or governments.

Since its inception, the unprecedented growth rate of Bitcoin is enough to attract the market participants' attention; between 2011 and 2015, Bitcoin rose more than 9,000%, from $4.60 to $426; in another time frame of April 27, 2015, to April 27, 2020, the price of Bitcoin went from $224 to

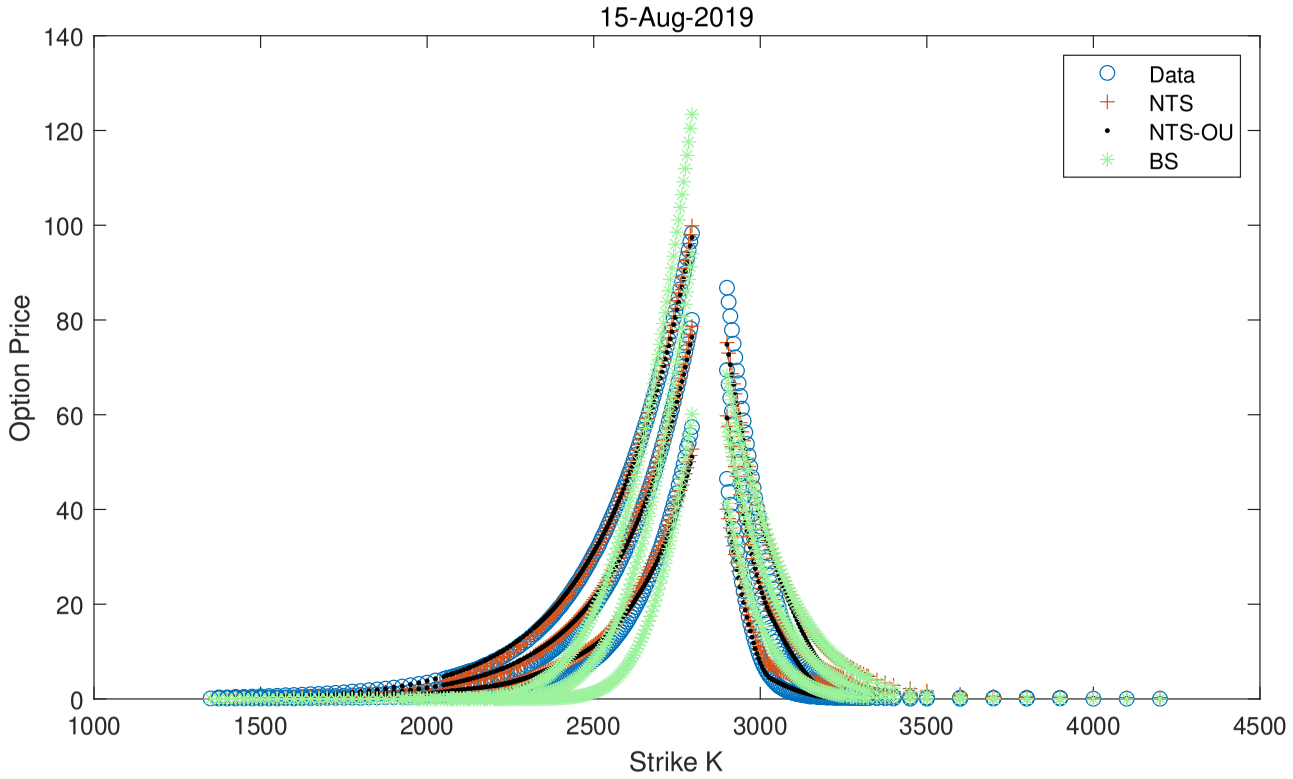

Figure 5: A term structure on the S&P 500 Index with the EUR-USD quanto option. Based on the RMSE, the BS model (18.9876) is clearly underperforms for all strike prices. The NTS model (10.173) is the next whereas the NTS-OU (6.4119) provides the best fitting capability.

Date	Model	RMSE	AAE	APE
05-Aug-2019	BS	9.3650	7.9902	0.2477
	NTS	3.4094	2.5545	0.0792
	NTS-OU	2.7870	2.1422	0.0664
08-Aug-2019	BS	8.6772	7.2288	0.3117
	NTS	3.4306	2.7598	0.1190
	NTS-OU	0.6912	0.5450	0.0235
13-Aug-2019	BS	9.3630	7.9459	0.3466
	NTS	2.0207	1.2874	0.0562
	NTS-OU	1.7385	1.3069	0.0570
15-Aug-2019	BS	18.9876	2.3157	6.3008
	NTS	10.1730	1.5348	4.1765
	NTS-OU	6.4119	1.5083	4.1037
21-Aug-2019	BS	7.2555	6.0643	0.3340
	NTS	3.8922	3.1852	0.1754
	NTS-OU	1.8426	1.4862	0.0819
23-Aug-2019	BS	8.1294	6.9202	0.3103
	NTS	4.1080	2.9506	0.1323
	NTS-OU	2.3988	1.8563	0.0832
26-Aug-2019	BS	8.8796	7.4992	0.2487
	NTS	4.1750	3.1249	0.1036
	NTS-OU	2.1491	1.7860	0.0592
27-Aug-2019	BS	8.9724	7.6249	0.2430
	NTS	3.7909	2.8799	0.0918
	NTS-OU	2.6298	2.0356	0.0649
29-Aug-2019	BS	9.0384	7.5591	0.2685
	NTS	1.5280	1.0059	0.0357
	NTS-OU	1.2946	1.0673	0.0379
30-Aug-2019	BS	9.5589	7.9193	0.2741
	NTS	1.3027	0.8250	0.0286
	NTS-OU	1.1596	0.9454	0.0327

Table 4: The goodness-of-fit test result for calibrated parameters shown in Table 3. This test is performed on the selected ten trading days in August 2019 for the S&P 500 Index and the EUR-USD quanto options. The NTS-OU consistently shows the lowest value on all test measures except for a few cases, while the BS model comprehensively underperforms.

$7,787.

However, as much as its profitability, its volatility has become a concern for investors. As a double-digit variance of the return is frequently observed in Bitcoin dynamics, Bitcoin is now considered as a high-risk asset. Indeed, it is now a well-known fact that Bitcoin clearly displays heavier tails than the market (see Kwon (2020)).

The other crucial factor to consider for Bitcoin derivatives pricing is its correlation with the equity market. At first, Bitcoin was called "digital gold" due to its fundamental similarities to gold and independent movement with the equity market. However, in recent years, whereas gold has still exhibited a strong negative correlation with the equity market, Bitcoin behavior has been more followed by the market trend. This contrast movement is more noticeable during economic turmoil. In other words, the dynamics of Bitcoin and the equity market are relatively low correlated when the market is in a normal regime, upon the market downturn starts, their correlation gauges up immediately.

In this example, we demonstrate the NTS-OU assumptions are effective to capture the features of the Bitcoin movement. As we mentioned earlier, this comes from the fact that Bitcoin has highly volatile returns with many outliers observed in the historical data. In addition to that, being a cryptocurrency, which is not tied to a particular government's monetary policy, makes the correlation less predictable in its pattern over time. Assuming a positive or a negative constant for correlation could be an unrealistic assumption as it often moves in a large degree and changes signs frequently. A detailed description of its correlation pattern will be described in Section 5.2.3.

We built a synthetic quanto option with the BTC-USD as its exchange

rate and DJIA to be the underlying index for this illustration and used the data from January 2015 to June 2020. Similarly to the previous example, we proxy the quanto option price by using the traded DJIA option prices (DIA). Then the payoff is given with a predetermined Bitcoin price (in Satoshi units). We follow the steps in previous sections to show that the NTS-OU has a superior performance in both physical and risk-neutral measures.

5.2.1 In sample test: fitting the DJIA and the BTC-USD

Both DJIA and Bitcoin daily log-return distribution is significantly leptokurtic with a large skew to the left, as indicated in its kurtosis and skewness in Table 5. The kurtosis for the DJIA is 27.9564 and for the Bitcoin is 17.2957. Given the convention that the normal distribution uses a kurtosis below 3, such a high kurtosis value could be challenging for other statistical distributions to capture its shape.

	DJIA	Bitcoin
Mean	2.7389×10^{-04}	0.0022
Standard Deviation	0.0125	0.0428
Skewness	-1.1219	-1.1268
Kurtosis	27.9564	17.2957
$Q_{.01}$	-0.1094	-0.2661
$Q_{.05}$	-0.0469	-0.1688
$Q_{.1}$	-0.0363	-0.1283
$Q_{.5}$	-0.0177	-0.0630
$Q_{.95}$	0.0147	0.0672
$Q_{.99}$	0.0313	0.1184
$Q_{.995}$	0.0483	0.1444
$Q_{.999}$	0.0917	0.2159

Table 5: Summary statistics for daily log-returns of the DJIA and the Bitcoin exchange rate from January 2015 to June 2020. The high kurtosis value far exceeding 3 (the normal distribution case) gives us the confidence to consider the NTS assumption.

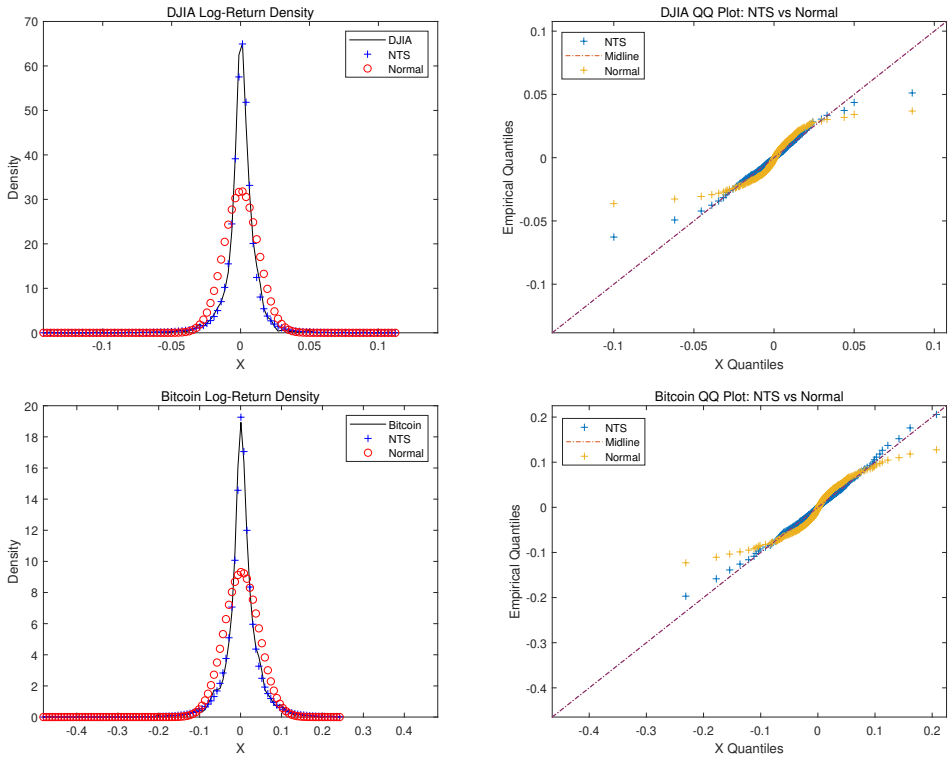

Figure 6: The log-return density distribution (left) and the Q-Q plot (right) for both the DJIA and the BTC-USD. The NTS distribution and the normal distribution are fitted. The empirical density shows the leptokurtic, and skewed nature. The Normal distribution does not account for the peakedness of the density distribution for both underlying assets. In the Q-Q plots, the NTS distribution shows a better fit than the normal distribution for all quantiles.

This can be visually seen in Figure 6, where the shape of the DJIA and the Bitcoin return distribution is hard to be described by the normal distribution simply with its mean and variance. On the other hand, the NTS is capable of tracking the return data closely. Both the fitted graph and the Q-Q plots demonstrate that the NTS accounts for the high peak in the middle as well as the heavier tails on both sides.

5.2.2 The Kolmogorov Smirnov (KS) Test

The KS test statistics for three candidate distributions are presented in Table 6 confirming that the NTS distribution calibrates successfully to the historical return distribution based on the p-value. For the normal distribution, in particular, the DJIA and Bitcoin's p-value of the KS statistics are both 1.0^{-4}, the null hypothesis is clearly rejected. On the other hand, the NTS displays a stark contrast by showing a high p-value of 0.8938 and 0.9995 for the DJIA and Bitcoin respectively. Given that the Bitcoin movements are volatile and have many outliers, it is not surprising that the NTS displays the best performance in fitting the empirical return distribution.

	DJIA		Bitcoin	
Distribution	KS Statistics	*p-value*	KS Statistics	*p-value*
Normal	0.1407	0.0001	0.1178	0.0001
Student's t	0.0228	0.4367	0.0251	0.3157
NTS	0.0101	0.8938	0.0057	0.9995

Table 6: p-values of the KS test for three candidate distribution in the DJIA and the BTC-USD at 5% of the significance level. The NTS displays the high p-value of 0.8938 and 0.9995 for both the DJIA and the Bitcoin movements whereas the normal assumption clearly fails to describe the empirical distribution.

5.2.3 Stochastic Correlation between the DJIA and the BTC-USD

As we remarked before, the correlation between Bitcoin and the DJIA is an interesting case; they loosely correlate generally, but upon the market regime switches, the correlation gauges up immediately. We can find this pattern in Figure 7 and the 4 spikes in the historical rolling correlation are directly related to the major market crashes; (1) June 2016: A major

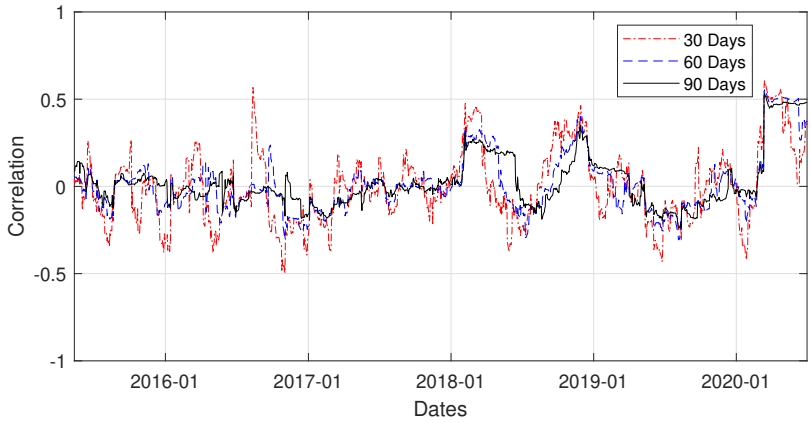

Figure 7: Historical rolling correlation between the DJIA and the BTC-USD returns over the period of January 2015 and June 2020.

stock sell-off event caused by the Brexit announcement which George Soros called, "a Black Friday for Britain." (2) January 2018: After a phenomenal bull run in 2017, the Bitcoin price fell off 65% in one month, which is known as the great crypto crash. (3) November 2018: The market capitalization of Bitcoin decreased below $100 billion for the first time since October 2017 and Bitcoin price declined to $5,500. (4) February 2020: This is a major stock market plunge caused by the COVID-19 outbreak. Major drops in DJIA and S&P 500 were recorded and world stock markets declined simultaneously out of the turmoil.

We ultimately show that capturing the stochastic correlation with the relaxed assumption on the constant correlation does provide added performance in the quanto option pricing under the risk-neutral measure.

5.2.4 Calibration to the quanto option

In this section, we present the calibration result with the goodness-of-fit measures for all three candidate models. We follow the same calibration

routine as described in the previous case study (see section 5.1.4), and use ten selected trading days in August 2019. The experiments are conducted with the DIA and the BTC-USD data.

Figure 8 shows that the fitting of three models to the proxy market data on August 8, 2019. In this case, due to the limited data points of DIA, the difference between the models is not much distinguishable. However, we note that the NTS model exhibits slightly better estimates on the out-of-the-money strikes. The performance of the NTS-OU model also can be confirmed by the goodness-of-fit measure; the RMSE of the BS model is 5.5368 whereas the NTS-OU model is 4.9258 respectively. (see Table 8).

To describe the model performance in detail, the calibrated parameters under the risk-neutral measures are provided in Table 7. The all estimated α parameter is below 2 which implies the existence of the heavy tails and the skewness in the underlying dynamics. Also, we can observe that the OU parameters display a relatively high value which gives us confidence in the capability of the OU parameters.

Moreover, as it can be consistently demonstrated in all three goodness of fit measures shown in Table 8, the NTS with stochastic dependence has more flexibility to calibrate to the market prices on selected nine trading days in August 2019. AAE, APE, and RMSE all have lower values for the NTS-OU compared to that of the NTS except for a few cases.

We also perform the same calibration and pricing performance testing to multiple expiries to demonstrate the model's flexibility in capturing the term structure. In Figure 9, we selected the expiry of 30 days and 120 days and fit the model to the price data. The deep-in-the-money options were removed. The term structure suggests NTS-OU has more adaptability than the BS or the NTS with constant correlation and this observation is

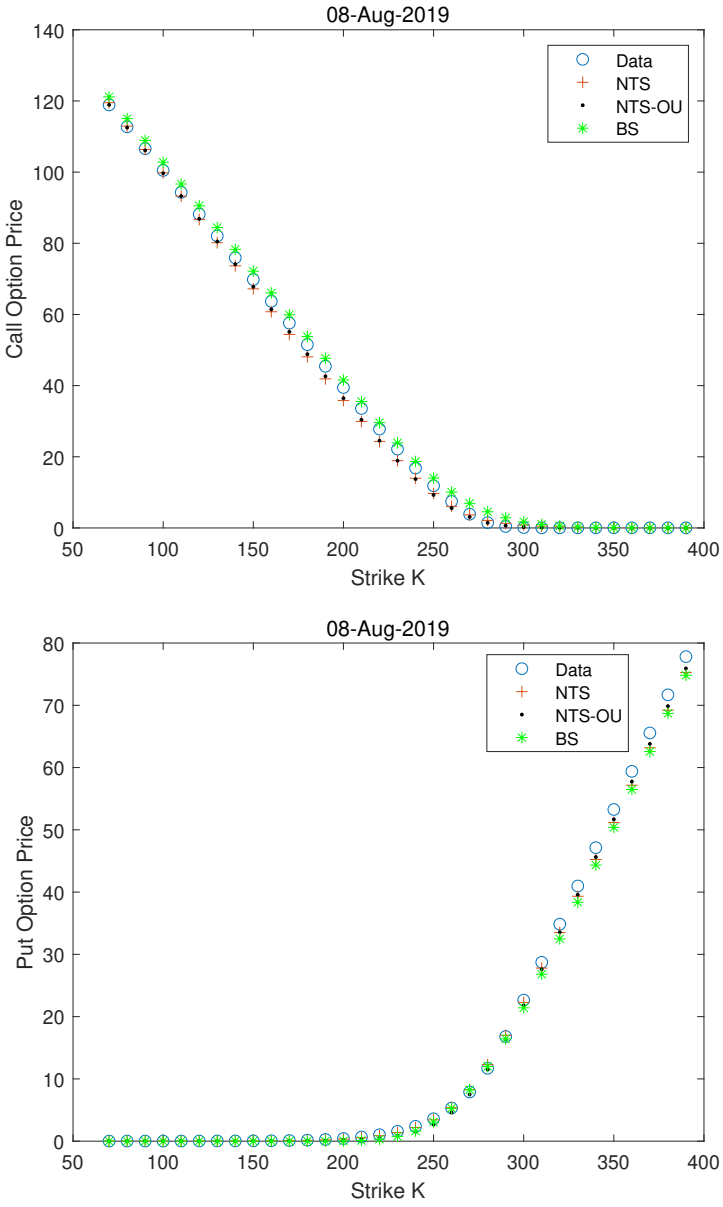

Figure 8: Comparing the estimated prices for the quanto option of the DIA with BTC-USD on August 8, 2019. Due to the limited data points, the difference between the NTS and the NTS-OU model is indistinguishable, but we note that the BS model does not perform well around the out-of-the-money strikes. The lower RMSE of the NTS-OU model (4.9258) than the BS model (5.5368) supports this observation.

Date	Model	α	θ	λ_Z	β_Z	σ_1	σ_2	μ_Z	ρ_0	σ_{OU}	κ_{OU}
05-Aug-2019	BS					0.1283	0.2042		0.6262		
	NTS	0.5920	2.3819	-0.0281	0.2152	0.1512	0.0931	0.0028			
	NTS-OU	0.6959	7.0222	-0.0111	0.2532	0.1485	0.0891	0.0011	-0.5891	2.4830	12.811
08-Aug-2019	BS					0.2238	0.1012		0.7847		
	NTS	0.6312	0.8274	-0.0170	0.0403	0.1508	0.0908	0.0017			
	NTS-OU	1.9012	8.2731	-0.0161	0.8061	0.0707	0.0663	0.0016	-0.3967	3.0990	11.0851
16-Aug-2019	BS					0.2308	0.1035		0.6984		
	NTS	0.7263	0.5895	-0.0148	0.0475	0.1186	0.0757	0.0015			
	NTS-OU	1.9530	8.3134	-0.0153	0.9111	0.0585	0.0554	0.0015	-0.3893	3.0982	11.0872
19-Aug-2019	BS					0.2255	0.1031		0.6977		
	NTS	0.8614	2.3498	-0.0119	0.1604	0.0983	0.0632	0.0012			
	NTS-OU	1.8874	9.5927	-0.0159	0.8433	0.0395	0.0347	0.0016	0.6865	3.3568	11.3882
20-Aug-2019	BS					0.2139	0.0893		0.7314		
	NTS	0.6478	0.8418	-0.0134	0.0430	0.1515	0.0903	0.0013			
	NTS-OU	1.8391	9.1712	-0.0162	0.3068	0.0879	0.0866	0.0016	0.9999	2.8940	11.7439
21-Aug-2019	BS					0.2230	0.0996		0.7858		
	NTS	0.4300	0.5422	-0.0172	0.0109	0.1519	0.0905	0.0017			
	NTS-OU	1.9182	9.1790	-0.0183	0.8845	0.0351	0.0212	0.0018	-0.2364	0.4304	12.3552
22-Aug-2019	BS					0.2235	0.0980		0.6994		
	NTS	0.6426	0.8374	-0.0162	0.0419	0.1515	0.0902	0.0016			
	NTS-OU	1.9459	9.3031	-0.0177	0.9298	0.0563	0.0541	0.0018	-0.0605	3.1438	13.2019
26-Aug-2019	BS					0.2573	0.1322		0.7773		
	NTS	0.6629	0.8505	-0.0166	0.0472	0.1524	0.0906	0.0017			
	NTS-OU	1.8713	9.5517	-0.0184	0.7822	0.0560	0.0339	0.0018	0.4611	0.1018	16.8824
27-Aug-2019	BS					0.2389	0.1009		0.7695		
	NTS	0.6696	0.8561	-0.0138	0.0475	0.1524	0.0906	0.0014			
	NTS-OU	1.8675	9.7971	-0.0172	0.8151	0.0773	0.0765	0.0017	0.9999	2.6241	12.6153

Table 7: Calibrated parameter comparison for the DJIA with Bitcoin quanto options between BS, NTS and NTS-OU.

consistent with the result of the goodness-of-fit test.

Date	Model	RMSE	AAE (bp[6])	APE (%)
05-Aug-2019	BS	8.9876	2.3157	6.3008
	NTS	5.0641	1.5348	4.1765
	NTS-OU	4.6683	1.5083	4.1037
08-Aug-2019	BS	5.5368	4.5863	3.3023
	NTS	1.8003	1.4018	1.2406
	NTS-OU	4.9258	3.8356	3.3946
16-Aug-2019	BS	7.0598	2.0326	4.8581
	NTS	4.4422	1.4505	3.4669
	NTS-OU	4.3475	1.4265	3.4094
19-Aug-2019	BS	6.9423	2.0062	5.0348
	NTS	3.2871	1.1909	2.9886
	NTS-OU	3.1332	1.1907	2.9882
20-Aug-2019	BS	6.8902	2.0123	4.9955
	NTS	4.7131	1.4260	3.5401
	NTS-OU	3.5251	1.2756	3.1666
21-Aug-2019	BS	5.6648	1.8138	4.2243
	NTS	5.0603	1.4871	3.4632
	NTS-OU	3.5799	1.2941	3.0137
22-Aug-2019	BS	7.4126	2.0804	4.8343
	NTS	5.3570	1.5183	3.5283
	NTS-OU	3.4812	1.2709	2.9534
26-Aug-2019	BS	6.9941	5.3094	0.4021
	NTS	1.5639	2.7305	0.2068
	NTS-OU	1.4490	2.8554	0.2162
27-Aug-2019	BS	5.3545	1.7804	4.1850
	NTS	5.4818	1.5694	3.6891
	NTS-OU	4.4516	1.4889	3.4998

Table 8: Quanto option price goodness of fit for DJIA with Bitcoin, The unit is in Bitcoin: RMSE, AAE, APE. Note that 05 August 2019 is run with multiple expiries to capture the term structure. The NTS-OU model shows the lowest RMSE, AAE, and APE with a few exceptions.

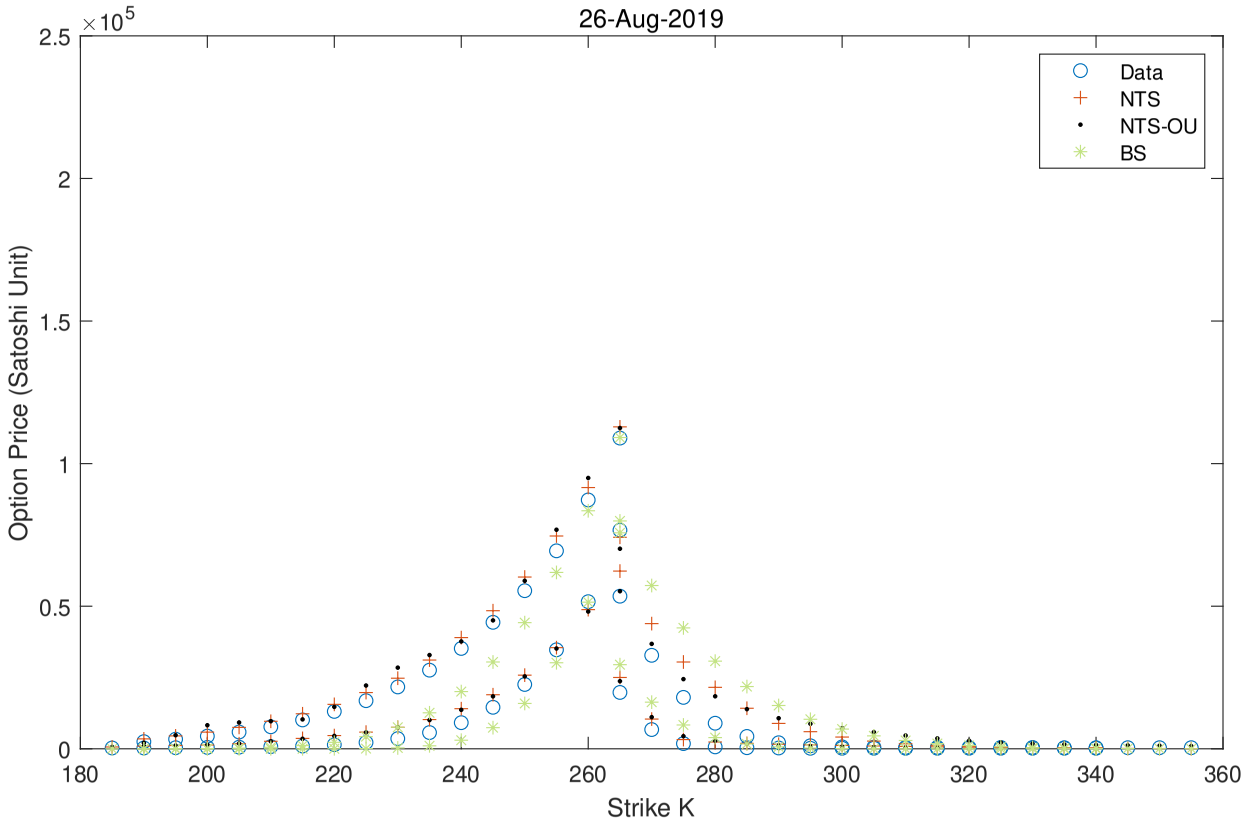

Figure 9: A term structure of the DIA and the BTC-USD quanto option with different expiries. We deleted the price of the deep in-the-money strikes.

6 Conclusion

A quanto option is traded in the over-the-counter market, so its price is decided by the consent of both parties based on the term-sheet rather than a market equilibrium. Hence, a robust theoretical model for its pricing is essential. The motivation of this study begins with the idea of establishing a more realistic pricing model that reflects the main empirical properties; heavy tails, skewness, and the stochastic correlation.

In this study, we proposed the NTS-OU pricing model for quanto options by combining the OU process with the previous NTS framework. We also found the risk-neutral measure by applying Girsanov's Theorem. Building on this, we finally derived the closed-form solution for a quanto option pricing model. For an effective numerical calculation, the characteristic function is provided to be directly used for fast Fourier Transform.

In the empirical illustration, we test two empirical case studies to understand the model performance in different market environments. For both case studies, across all selected trading dates, the NTS-OU model consistently displayed a superior price estimation than the BS model and the NTS model. This conclusion is supported by the statistical summary, multiple goodness-of-fit metrics, and the term structure.

Meanwhile, it should be noted that the NTS-OU framework can be applied to model multi-asset option pricing or generally any models that have a stochastic correlation. A quanto option pricing is a bivariate example of the NTS-OU framework, but it can be used for higher-dimensional examples.

As the next subject, we can investigate the hedging strategy for the NTS-OU quanto option model. Derivatives are utilized as a hedging tool

for traders. The most challenging part for the NTS based model is deriving a hedging strategy. The NTS process as one of a Lévy process allows jumps and this is not deleted by delta hedging. Many alternatives are suggested such as local risk-minimizing hedging by Boyarchenko *et al.* (2002) and this can be applied for the NTS-OU model. This will be the subject of future study.

Another subject regarding the NTS-OU model is investigating the trade-off between flexibility by adding parameters and computational effectiveness. Finding an optimal point between flexibility and accuracy would be an important study for the application of the NTS-OU model.

References

Barndorff-Nielsen, O. E. and Shephard, N. (2001). Non-gaussian ornstein–uhlenbeck-based models and some of their uses in financial economics. *Journal of the Royal Statistical Society: Series B (Statistical Methodology)*, *63*(2), 167–241.

Barndorff-Nielsen, O. E., Shephard, N., *et al.* (2001). *Normal modified stable processes*. MaPhySto, Department of Mathematical Sciences, University of Aarhus Aarhus.

Baxter, M., Rennie, A., and Rennie, A. J. (1996). *Financial calculus: an introduction to derivative pricing*. Cambridge university press.

Bertoin, J. (1996). *Lévy processes*, vol. 121. Cambridge university press Cambridge.

Black, F., Derman, E., and Toy, W. (1990). A one-factor model of interest rates and its application to treasury bond options. *Financial Analysts Journal*, *46*(1), 33–39.

Black, F. and Scholes, M. (1973). The pricing of options and corporate liabilities. *Journal of political economy*, *81*(3), 637–654.

Boyarchenko, S. and Levendorskii, S. (2000). Option pricing for truncated Lévy processes. *International Journal of Theoretical and Applied Finance*, *03*(03), 549–552.

Boyarchenko, S., Levendorskii, S., *et al.* (2002). Barrier options and touch-and-out options under regular Lévy processes of exponential type. *The Annals of Applied Probability*, *12*(4), 1261–1298.

Carr, P., Geman, H., Madan, D. B., and Yor, M. (2002). The fine structure of asset returns: An empirical investigation. *The Journal of Business*, *75*(2), 305–332.

Carr, P., Geman, H., Madan, D. B., and Yor, M. (2003). Stochastic volatility for lévy processes. *Mathematical finance*, *13*(3), 345–382.

Carr, P. and Wu, L. (2004). Time-changed Lévy processes and option pricing. *Journal of Financial economics*, *71*(1), 113–141.

Clark, P. K. (1973). A subordinated stochastic process model with finite variance for speculative prices. *Econometrica: journal of the Econometric Society*, 135–155.

Cont, R. and Tankov, P. (2004). Nonparametric calibration of jump-diffusion option pricing models.

Duan, J.-c. and Wei, J. z. (1999). Pricing foreign currency and cross-currency options under GARCH. *The Journal of Derivatives*, *7*(1), 51–63.

Gerber, H. and Shiu, E. (1994). Option pricing by esscher transforms. *Transactions of Society of Actuaries*, *46*, 99–140.

Grigelionis, B. (1999). Processes of meixner type. *Lithuanian Mathematical Journal*, *39*(1), 33–41.

Huang, S.-C. and Hung, M.-W. (2005). Pricing foreign equity options under Lévy processes. *Journal of Futures Markets: Futures, Options, and Other Derivative Products*, *25*(10), 917–944.

Jäckel, P. (2016). Quanto skew. URL `https://jaeckel.000webhostapp.com/QuantoSkew.pdf`. White Paper.

Ken-Iti, S. (1999). *Lévy processes and infinitely divisible distributions*. Cambridge university press.

Kim, Y. S. (2005). *The modified tempered stable processes with application to finance*. Ph.D. thesis.

Kim, Y. S., Lee, J., Mittnik, S., and Park, J. (2015). Quanto option pricing in the presence of fat tails and asymmetric dependence. *Journal of Econometrics*, *187*(2), 512 – 520.

Kim, Y. S., Rachev, S., Dong, M., and Chung, D. (2006). The modified tempered stable distribution, GARCH models and option pricing. *Probability and Mathematical Statistics*, *29*.

Kim, Y. S., Rachev, S. T., Bianchi, M. L., and Fabozzi, F. J. (2008). Financial market models with Lévy processes and time-varying volatility. *Journal of Banking Finance*, *32*(7), 1363 – 1378.

Kim, Y. S., Rachev, S. T., Bianchi, M. L., and Fabozzi, F. J. (2009). A new tempered stable distribution and its application to finance. In *Risk Assessment*, Springer. 77–109.

Klebaner, F. C. (2005). *Introduction to stochastic calculus with applications*. World Scientific Publishing Company.

Koponen, I. (1995). Analytic approach to the problem of convergence of truncated lévy flights towards the gaussian stochastic process. *Physical Review E*, *52*(1), 1197.

Kwon, J. H. (2020). Tail behavior of bitcoin, the dollar, gold and the stock market index. *Journal of International Financial Markets, Institutions and Money*, *67*, 101202.

Lewis, A. L. (2001). A simple option formula for general jump-diffusion and other exponential lévy processes. *Available at SSRN 282110*.

Linders, D. and Schoutens, W. (2014). A framework for robust measurement of implied correlation. *Journal of Computational and Applied Mathematics*, *271*, 39 – 52.

Ma, J. (2009). Pricing foreign equity options with stochastic correlation and volatility. *Annals of Economics and Finance*, *10*, 303–327.

Madan, D. and Yor, M. (2006). Cgmy and meixner subordinators are absolutely continuous with respect to one sided stable subordinators. *arXiv preprint math/0601173*.

Mandelbrot, B. (1963). New methods in statistical economics. *Journal of political economy*, *71*(5), 421–440.

Menn, C. and Rachev, S. T. (2009). Smoothly truncated stable distributions, GARCH-models, and option pricing. *Mathematical Methods of Operations Research*, *69*(3), 411.

Mittnik, S., Paolella, M. S., and Rachev, S. T. (2000a). Diagnosing and treating the fat tails in financial returns data. *Journal of Empirical Finance*, *7*(3-4), 389–416.

Mittnik, S., Paolella, M. S., and Rachev, S. T. (2000b). Diagnosing and treating the fat tails in financial returns data. *Journal of Empirical Finance*, *7*(3-4), 389–416.

Monroe, I. (1978). Processes that can be embedded in brownian motion. *The Annals of Probability*, 42–56.

Patton, A. J. (2006). Modelling asymmetric exchange rate dependence. *International economic review*, *47*(2), 527–556.

Rachev, S. T., Menn, C., and Fabozzi, F. J. (2005). *Fat-tailed and skewed asset return distributions: implications for risk management, portfolio selection, and option pricing*, vol. 139. John Wiley & Sons.

Rachev, S. T. and Mittnik, S. (2000). *Stable Paretian models in finance*, vol. 7. Wiley.

Rosiński, J. (2007). Tempering stable processes. *Stochastic processes and their applications*, *117*(6), 677–707.

Schoutens, W. (2002). *The Meixner process: Theory and applications in finance*. Eurandom Eindhoven.

Teng, L., Ehrhardt, M., and Günther, M. (2015). The pricing of quanto options under dynamic correlation. *Journal of Computational and Applied Mathematics*, *275*, 304–310.

A Appendix

A.1 Calibration Results for Quanto Option of the S&P 500 Option and the EUR-USD Exchange Rate

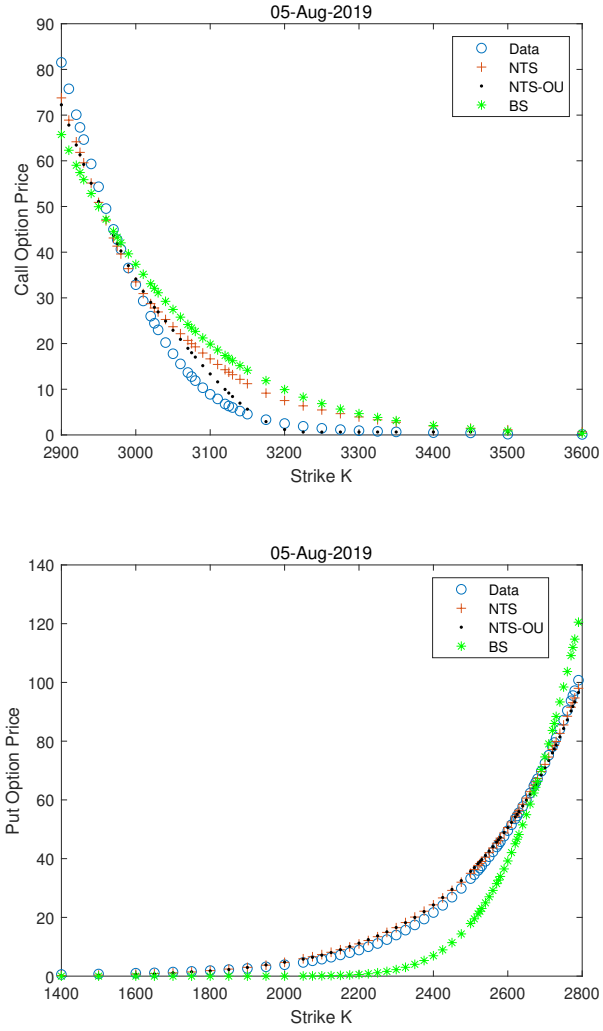

Figure 10: Quanto option pricing results - 05 August 2019

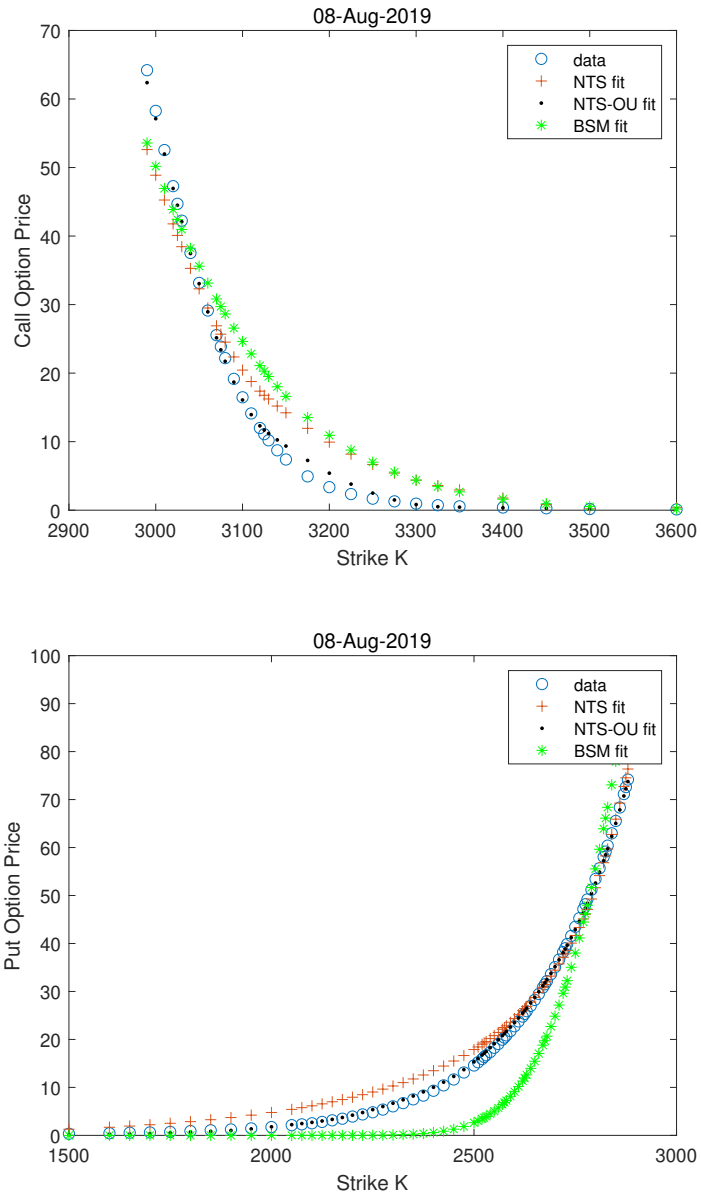

Figure 11: Quanto option pricing results - 08 August 2019

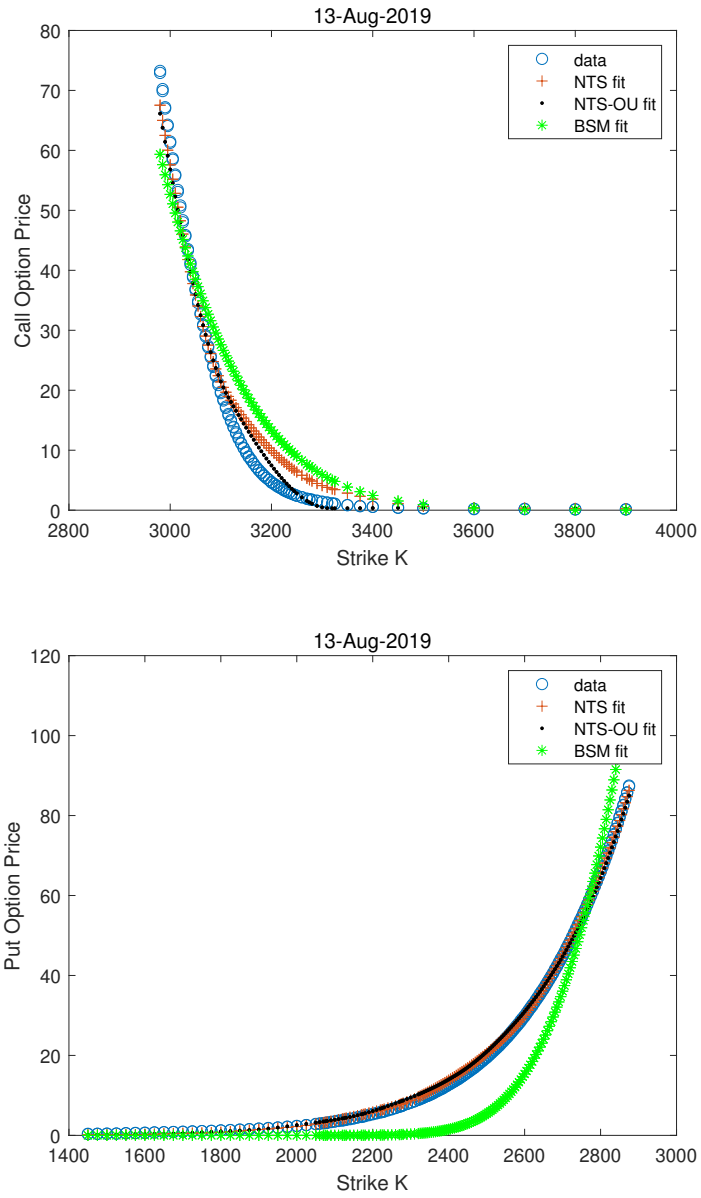

Figure 12: Quanto option pricing results - 13 August 2019

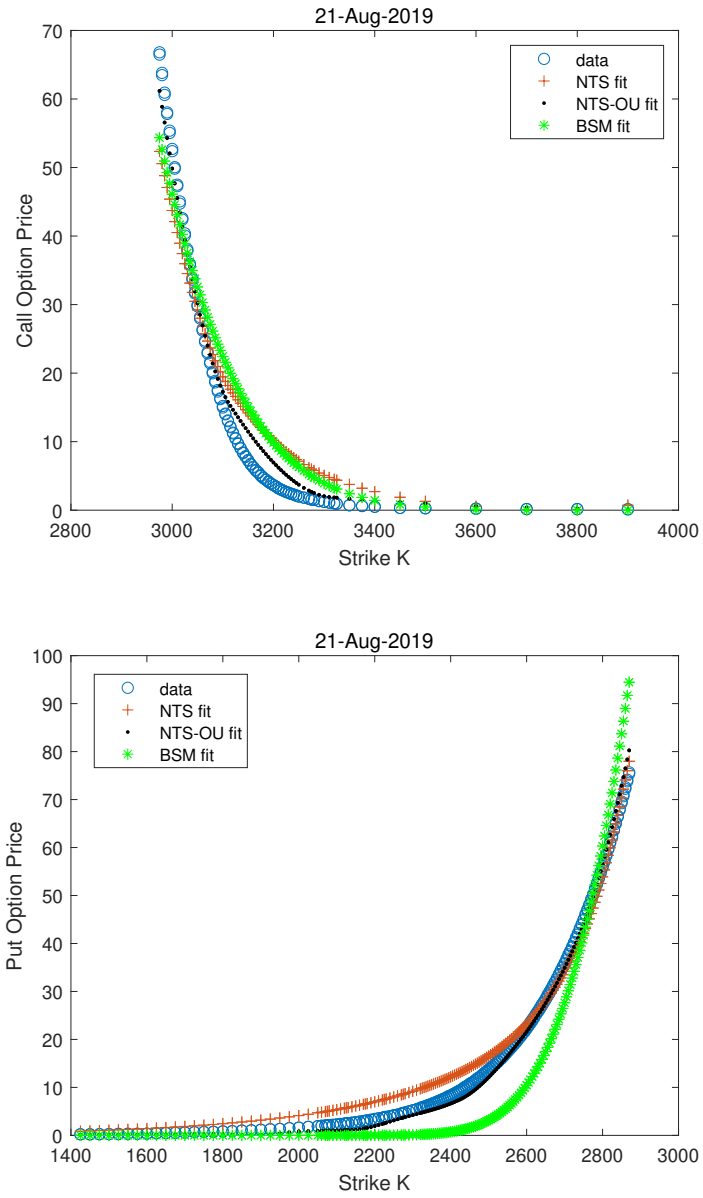

Figure 13: Quanto option pricing results - 21 August 2019

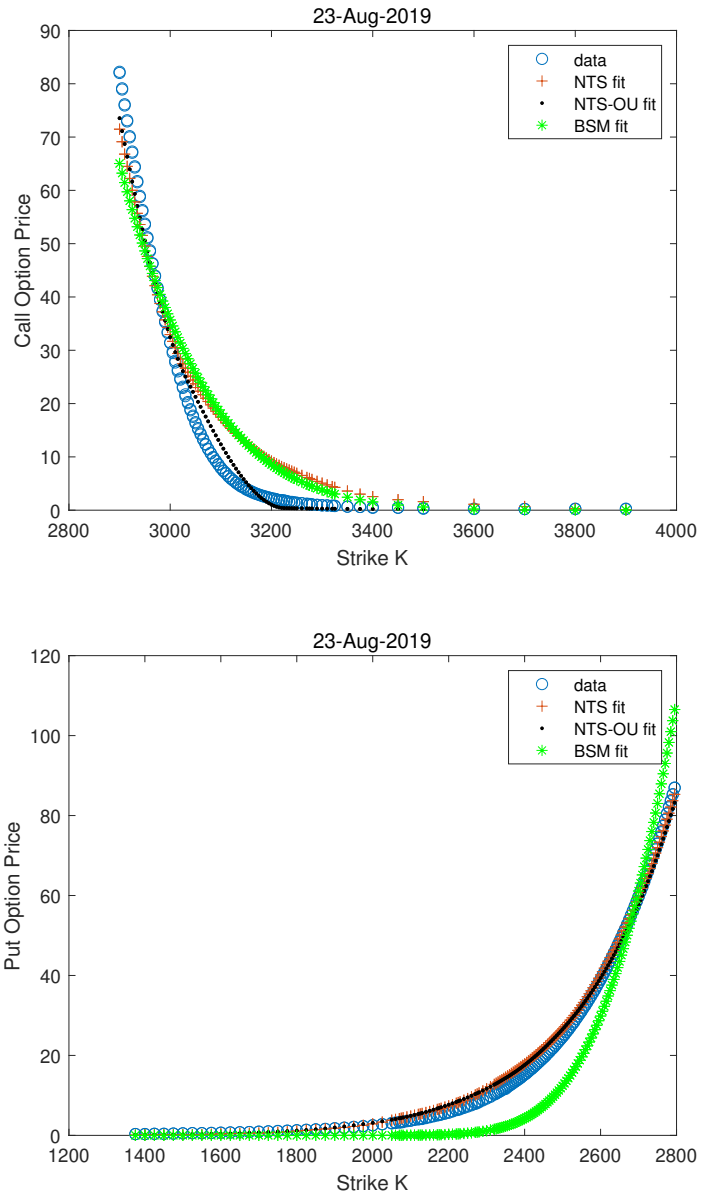

Figure 14: Quanto option pricing results - 23 August 2019

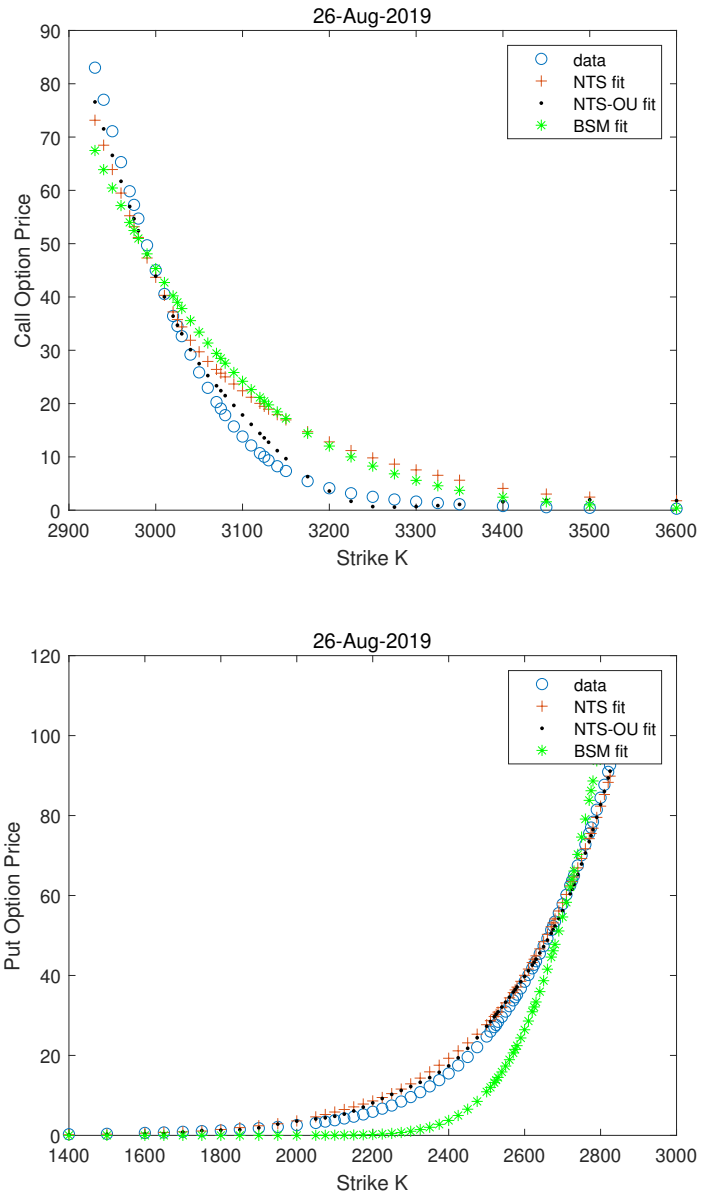

Figure 15: Quanto option pricing results - 26 August 2019

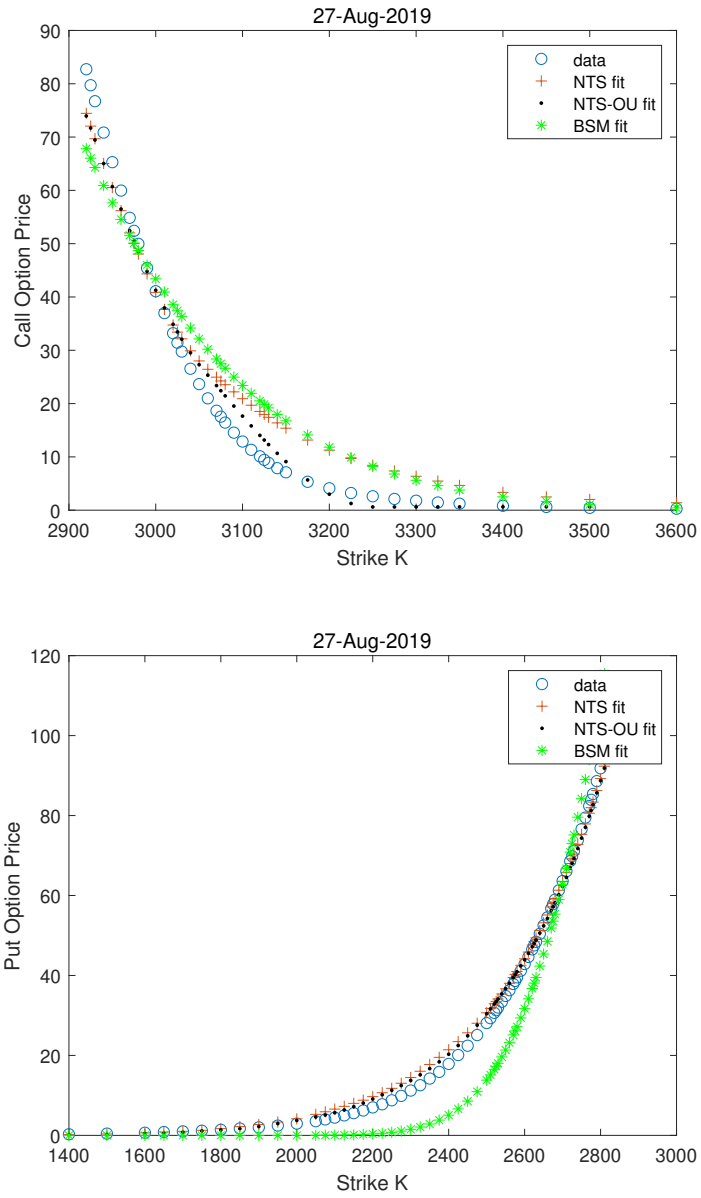

Figure 16: Quanto option pricing results - 27 August 2019

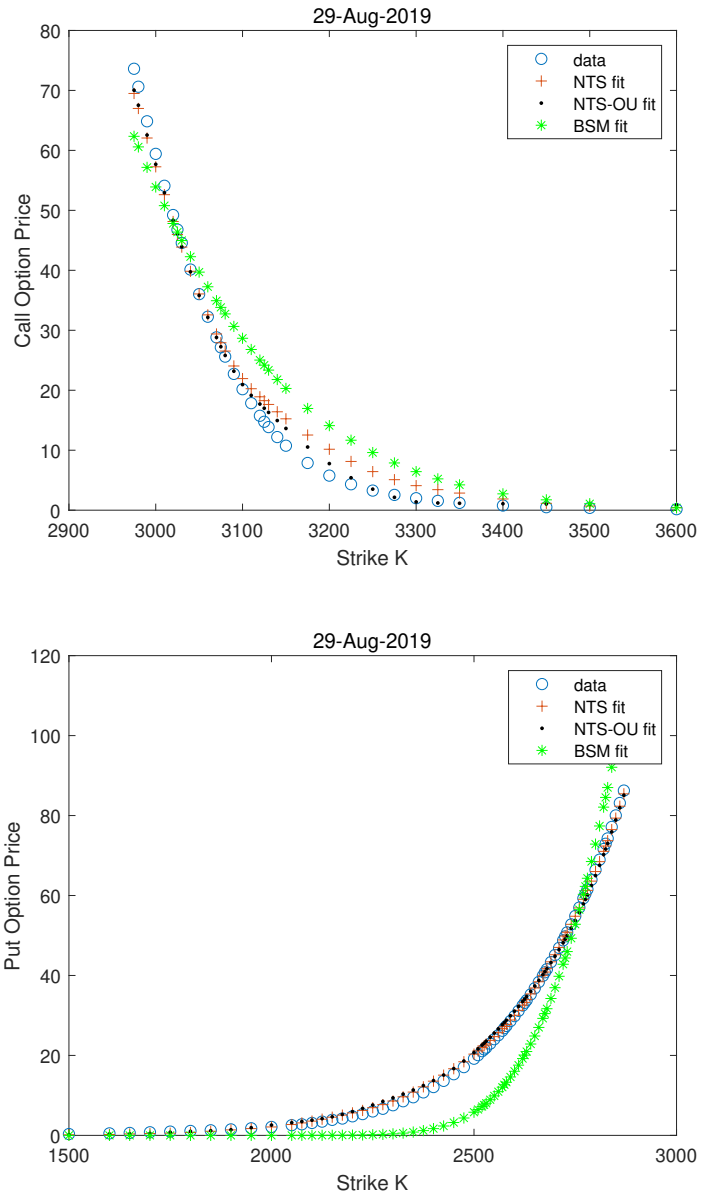

Figure 17: Quanto option pricing results - 29 August 2019

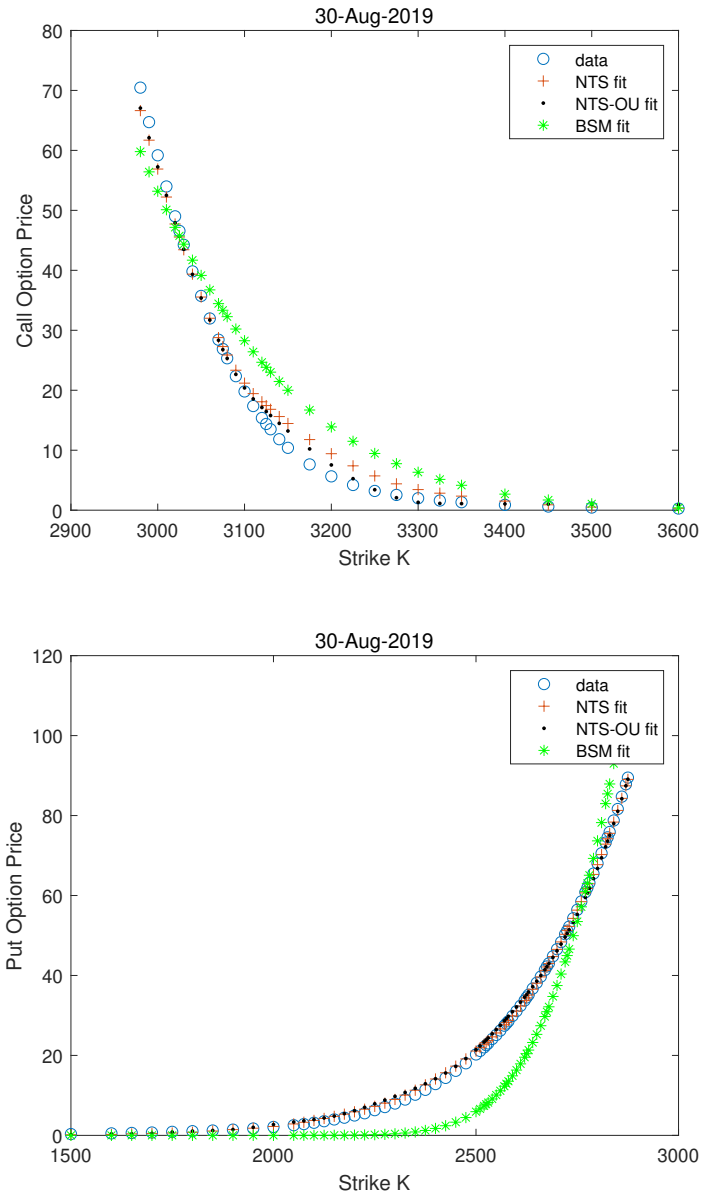

Figure 18: Quanto option pricing results - 30 August 2019

A.2 Calibration Results for Quanto Option of the DJIA Option and the BTC-USD Exchange Rate

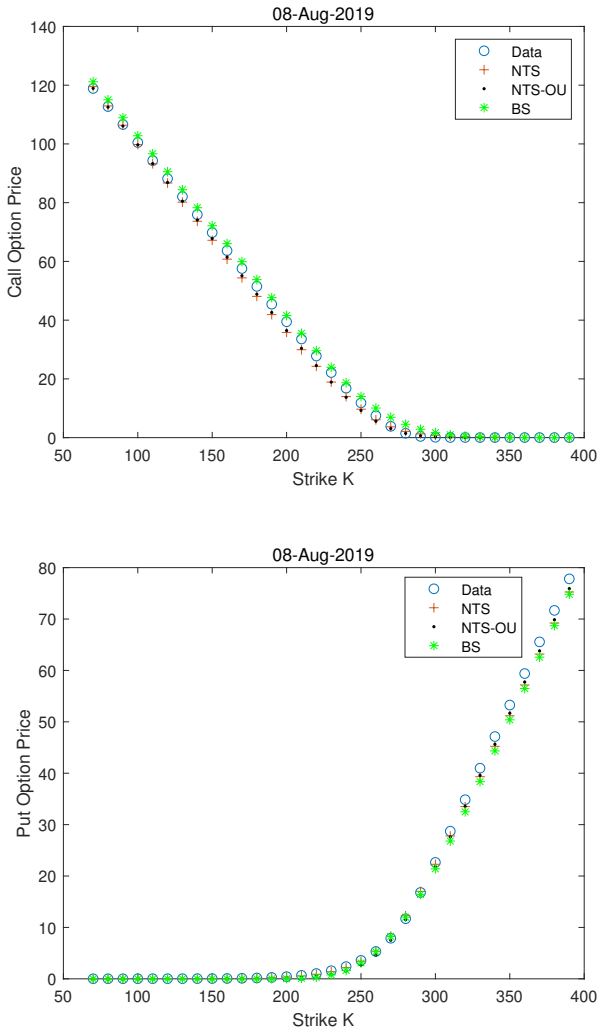

Figure 19: Quanto option pricing results - 08 August 2019

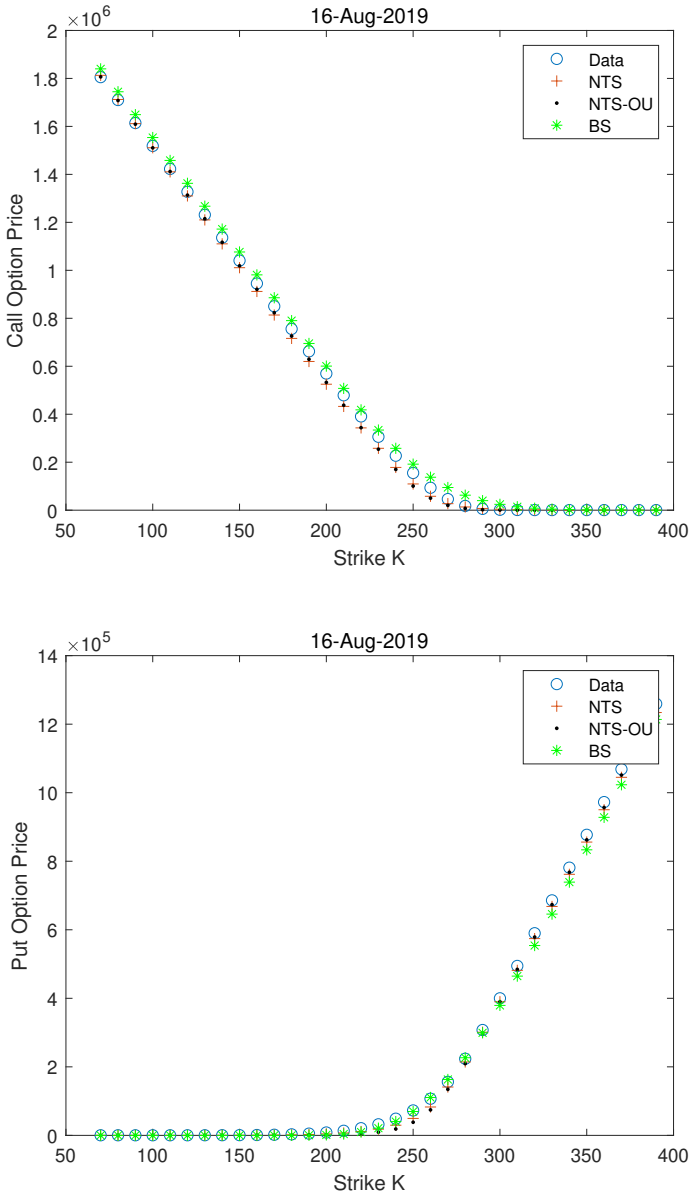

Figure 20: Quanto option pricing results - 16 August 2019

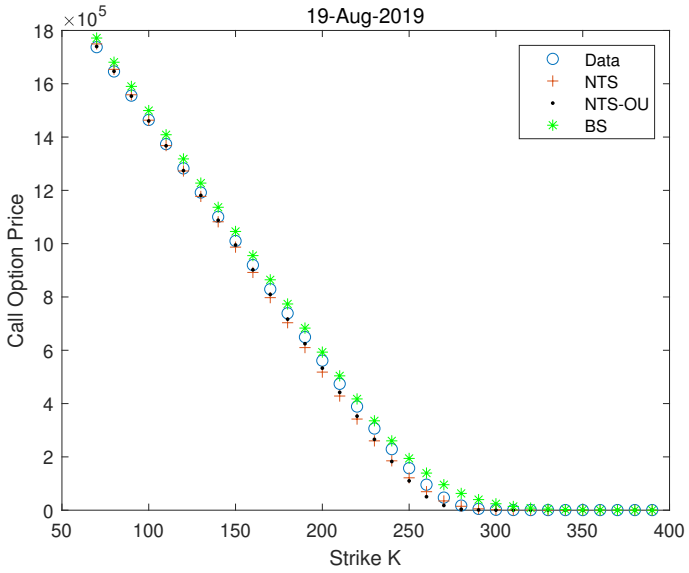

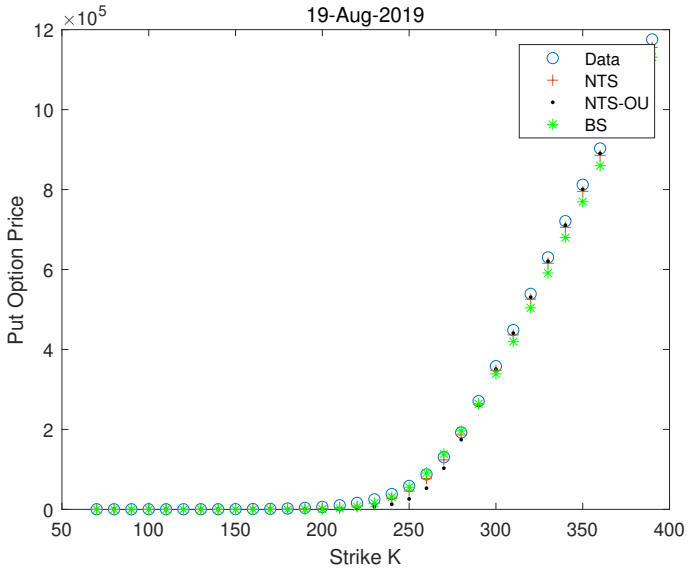

Figure 21: Quanto option pricing results - 19 August 2019

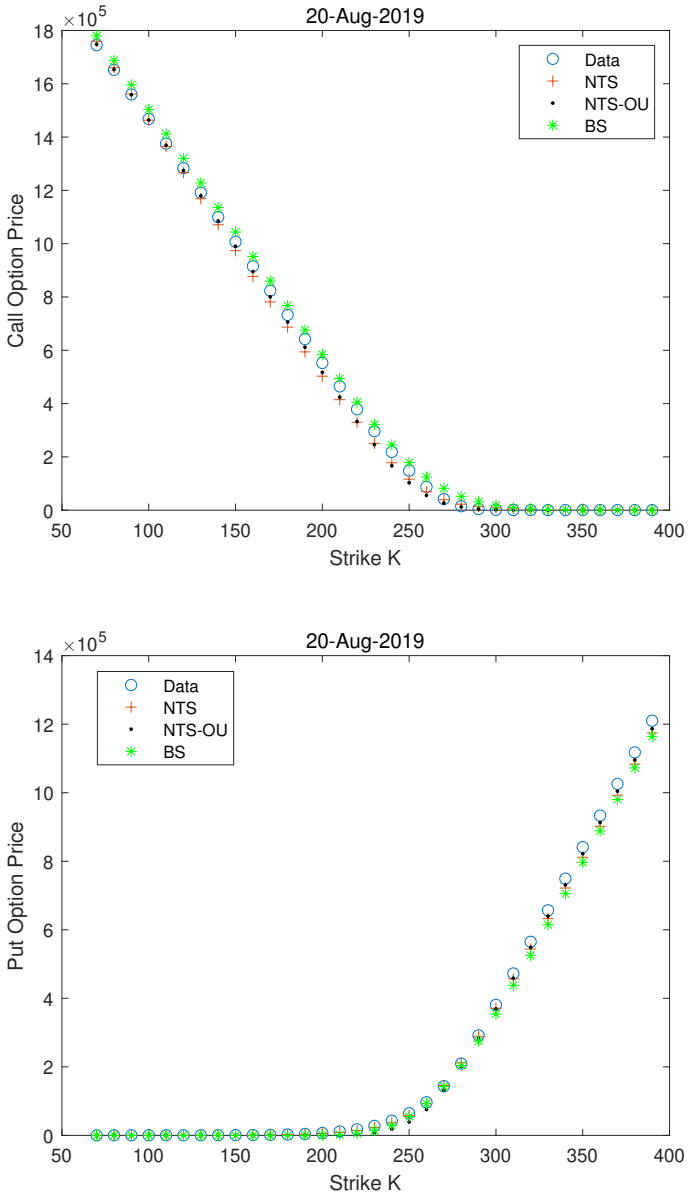

Figure 22: Quanto option pricing results - 20 August 2019

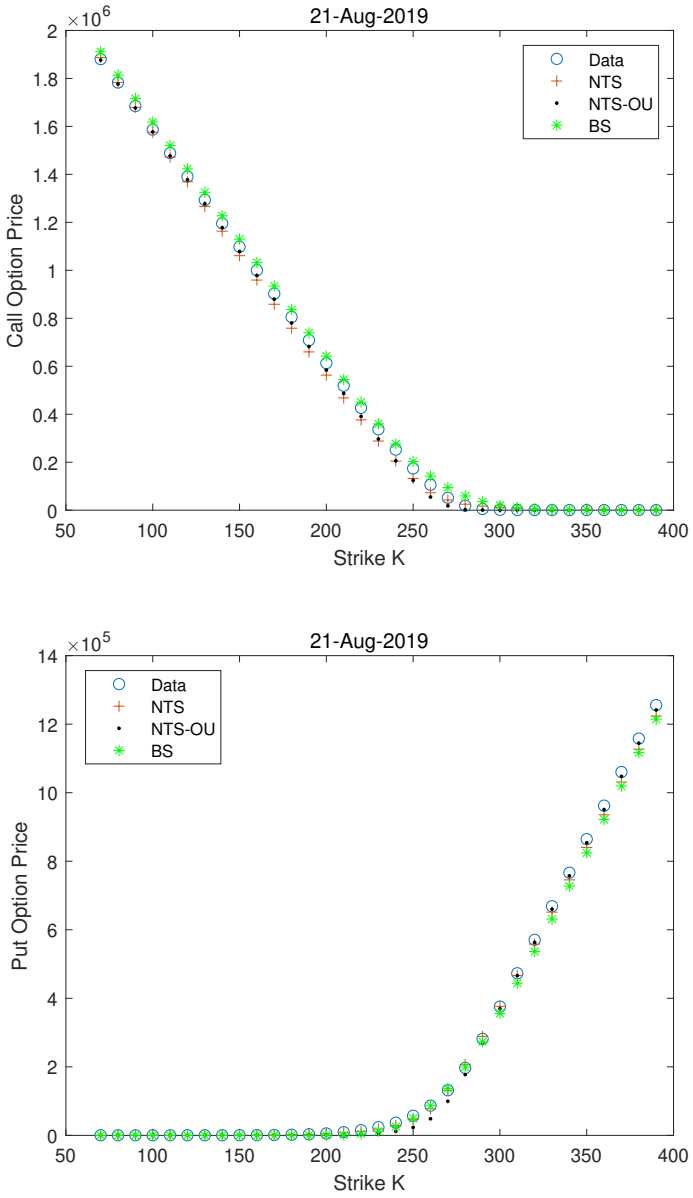

Figure 23: Quanto option pricing results - 21 August 2019

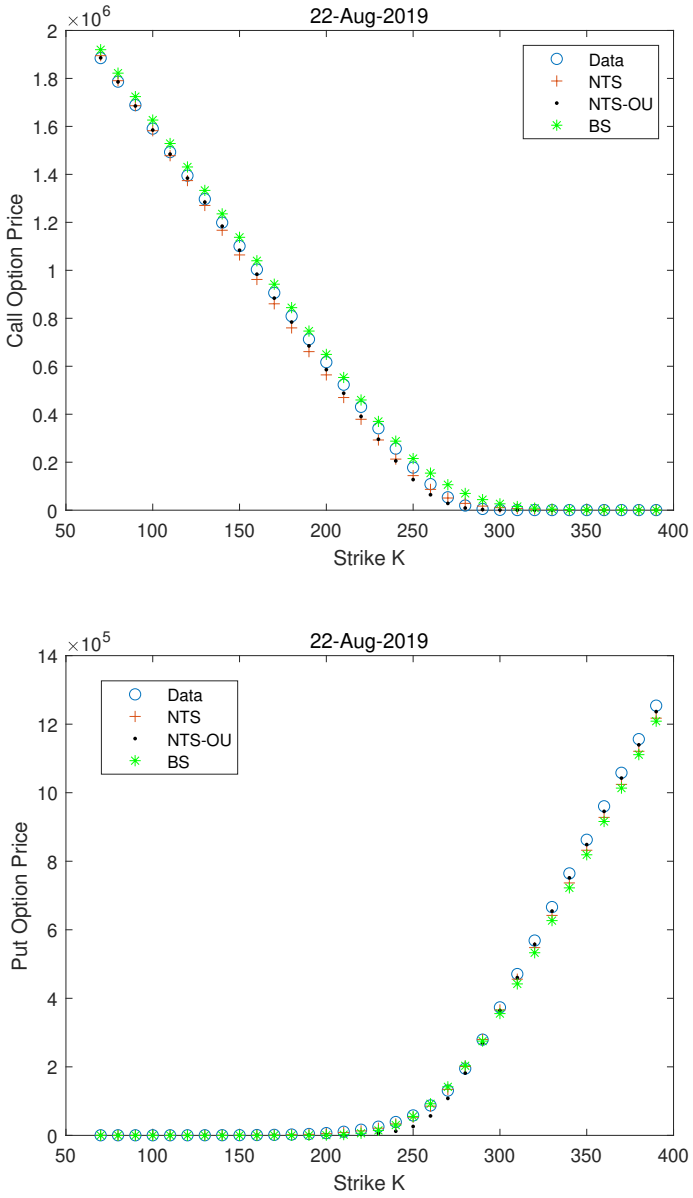

Figure 24: Quanto option pricing results - 22 August 2019

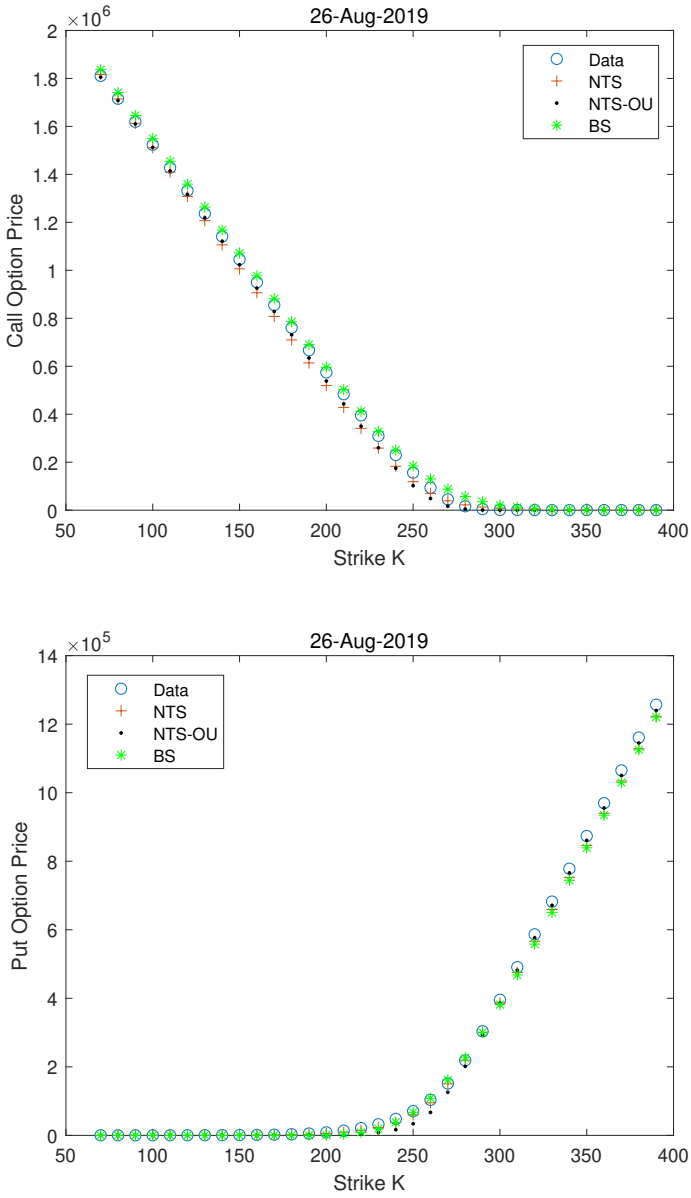

Figure 25: Quanto option pricing results - 26 August 2019

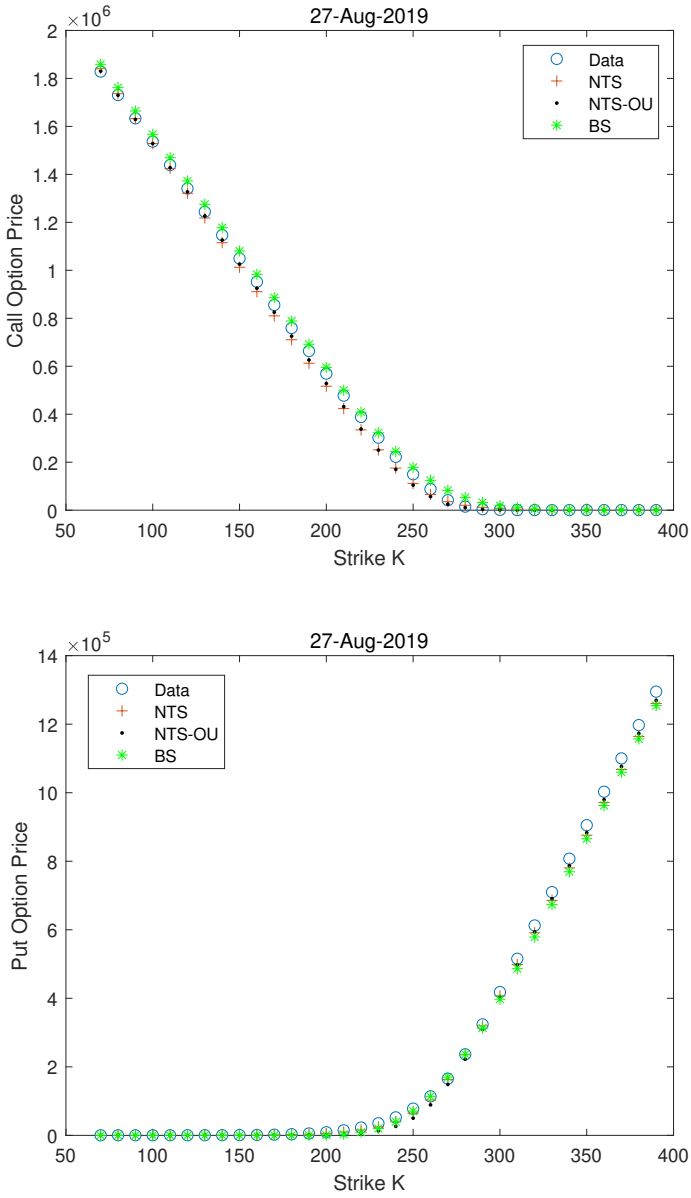

Figure 26: Quanto option pricing results - 27 August 2019